A Design Methodology for Hysteretic Dampers in Buildings under Extreme Earthquakes

by

Cody H. Fleming

B.S., Hope College, MI (2003)

Submitted to the Department of Civil and Environmental Engineering in partial fulfillment of the requirements for the degree of

Master of Engineering in Civil and Environmental Engineering
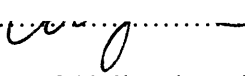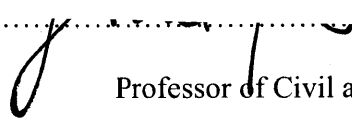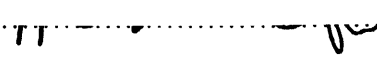
at the

MASSACHUSETTS INSTITUTE OF TECHNOLOGY

June 2004

© 2004 Cody H. Fleming. All rights reserved.

The author hereby grants to MIT permission to reproduce and to distribute publicly paper and electronic copies of this thesis document in whole or in part.

Signature of Author...
Cody H. Fleming
Department of Civil and Environmental Engineering
May 7, 2004

Certified by...
Jerome J. Connor
Professor of Civil and Environmental Engineering
Thesis Supervisor

Accepted by...
Heidi Nepf
Chairman, Departmental Committee on Graduate Students
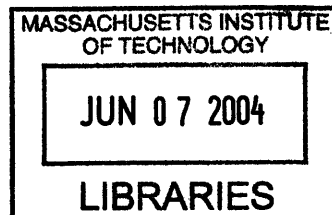
A Design Methodology for Hysteretic Dampers in Buildings under Extreme Earthquakes

by

Cody H. Fleming

Submitted to the Department of Civil and Environmental Engineering on
May 7, 2004 in partial fulfillment of the requirements for the degree of
Master of Engineering in Civil and Environmental Engineering

Abstract

This research proposes a design methodology for hysteretic dampers in buildings under high levels of seismic hazard. Developments in structural materials have led to designs that satisfy strength requirements but are often very flexible. This trend, along with increasingly stringent building performance criteria, suggests a philosophy of controlling structural motion as opposed to merely designing for strength, particularly when related to earthquake design. Included in this thesis is a design algorithm that calibrates stiffness and yield force level, two controlling parameters in the implementation of hysteretic dampers, in order to obtain optimal structural response under two levels of earthquake severity. In addition, a parametric study illustrates the merits and drawbacks of various stiffness and yield force allocations.

Thesis Supervisor: Jerome J. Connor
Title: Professor of Civil and Environmental Engineering

Acknowledgments

Contents

List of Figures and Tables

Chapter 1

State of the Art

Current design codes require that a building have sufficient strength to resist certain loads or load combinations [1]. The ASCE specifies that a building meet three basic requirements: strength, serviceability, and self-straining forces. All loads and load combinations result from the weight of the building materials and occupants, environmental effects, and differential movement. In the case of earthquake design, an equivalent static force is applied to the building, and is calculated via a multitude of factors, including geographic region and occupancy importance. Depending on the height of the building, the force can be distributed throughout the height, relative to the amount of mass the structure is supporting at that given height.

This approach is flawed for several reasons. First, the code gives little regard to the possible motion implied by the forces a building experiences. This has numerous ramifications, including the limited amount of acceleration that humans and certain machinery can operate under, and the fact that large displacements can cause building materials to go beyond their elastic design limit. The second fundamental flaw of this design approach regards the lack of dynamic analysis under earthquake and other dynamic loading conditions. One could design a building with ample resistance to earthquake forces but with a fundamental period closely matching those of earthquakes that represent the geography in which the building resides. It has been shown by Jerome J. Connor[1] in [2] and in countless other textbooks and journal articles that an excitation with a period equal to or near the fundamental frequency of the building will greatly magnify the motion of said building. The following figure shows the response of a structure at resonance, or when the frequency of the excitation equals the frequency of the structure. This kind of motion could be severely detrimental to a building.

---

[1] Massachusetts Institute of Technology, United States

$$p = \frac{\Omega}{\omega} = \Omega \sqrt{\frac{m}{k}}$$
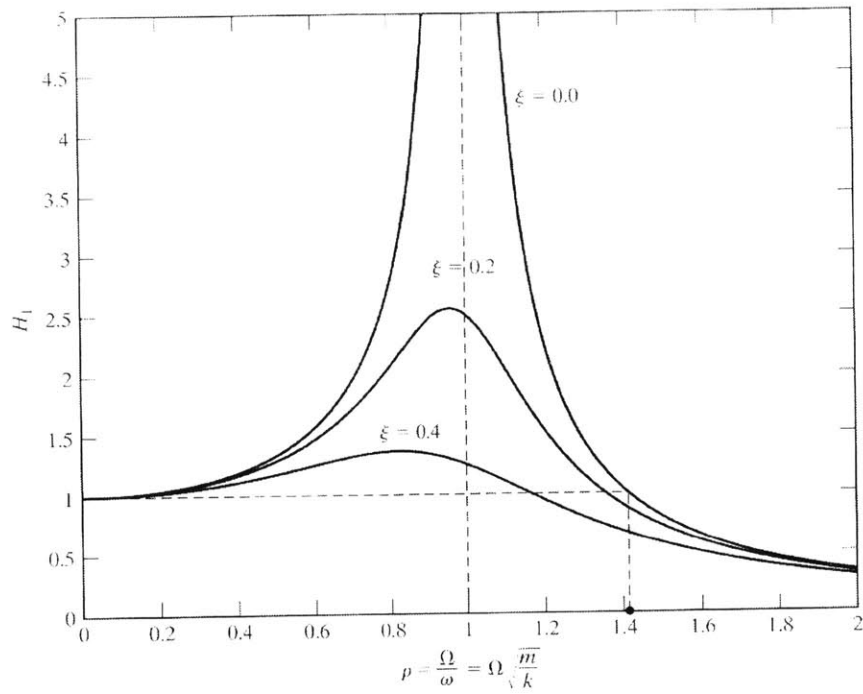
Figure 1-1: Illustration of Resonance [2]

This argument should sufficiently demonstrate the inadequacy of certain design codes for earthquake design. In this thesis, a different design approach is pursued in which motion is the chief design constraint.

Chapter 2

Introduction to the Motion Based Design Philosophy

Given the advancement in technology, engineers have been able to design taller buildings and longer span horizontal structures, which tend to have greater deflections under service loads [2]. It has already been suggested above that current building codes give little regard to motion as a design parameter. This, combined with an increase in repair and insurance costs suggests a new design trend [4]. "Since damage is due to structural motion, damage control is achieved through the control of structural motion." [3] This paradigm seeks to limit the amount of damage a structure experiences under intense dynamic loads. This discussion gives rise to two questions. Given the increase in repair and insurance costs, how does one assess the increased costs associated with designing in a new way and how does this relate to the overall economics of a building, i.e. life cycle analysis, initial project cost, etcetera? Secondly, when designing to control motion and subsequently to control damage, what level of implied damage is acceptable? Not only do these questions have direct effect on design and economics; a personal component is also revealed, as in, what about the safety and comfort of the structure's occupants or users? Comfort is typically neglected for seismic design, however, with safety being the foremost consideration.

2.1 Cost

Two factors can be associated with the cost of a civil project. One is the initial project cost, or how much money is required for the structure to be built. The second pertains to the life cycle of the building, as in revenues associated with use, maintenance, efficiency, and end-of-use aspects. This thesis focuses on issues related to damage, which could result in large maintenance or repair costs, or complete building failure, which is obviously quite expensive to the owner. While it does cost more to use a damage control

design method, Figure 2-1 schematically illustrates the economic benefits of building a Damage Controlled Structure.
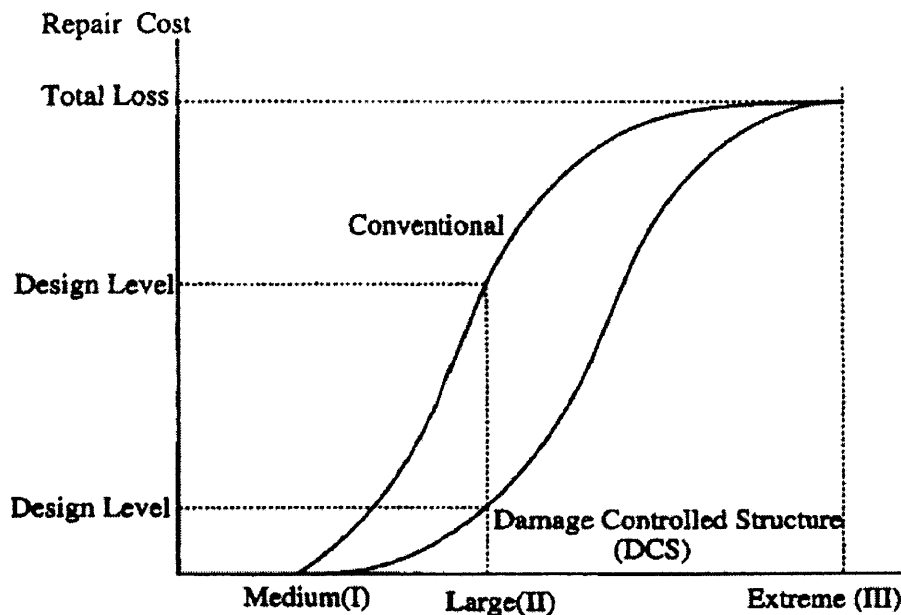
Figure 2-1: Repair Costs for Different Design Schemes [3]

This figure is intimately related to the study of the life cycle of a building, and in order to cause a paradigm shift towards motion-based design, the culture of both designers and owners must change. It has been shown that only 60 percent of designers undertake some form of cost analysis, and many of these studies only consider initial construction costs [10]. In addition, fewer than 50 percent of owners partake in cost analysis studies, again many of which do not take into account possible repair costs under an extreme event. Huge economic losses can and have occurred due to intense earthquakes, but perhaps a more important *cost* factor should also be considered: human safety. "Lessons learned from the Hyogoken-Nanbu Earthquake and the Northridge Earthquake indicated that...failures in the welded connections between beams and columns resulted not only in huge economic loss but also the loss of human lives. " [6]

There exists a slight dichotomy in terms of how designers and owners view construction costs. While those involved in construction projects seem reluctant to be involved in cost analyses, particularly those related to the benefits of a damage controlled structure, there is a premium associated with using current passive damping technologies (which apply directly to damage controlled structures). Designers place a 5.8 percent cost premium relative to total structural cost on using current passive damping technologies, while owners place a 5.4 percent premium on such uses. Furthermore, designers and owners place upwards of 7.2 percent cost premium for the use of *new technologies* [10]. This is an important consideration when investigating a novel design methodology and will be explored later in a cost analysis of the results of this research. With a brief introduction to the possible economic benefits and barriers of motion based design, or "Damage Controlled Structures" in the nomenclature of Connor and Wada used above, it is now logical to investigate the proper design levels for acceptable damage.

2.2 Performance Levels

Work has been done recently by the Federal Emergency Management Agency (FEMA) to create a widely accepted and technically sound guideline for designing buildings or assessing existing buildings, which could experience seismic activity. The most fundamental goal of any engineer is to prevent the complete collapse of a building. However, it was shown previously that the reduction in the damage level of a building is not only economical in the long term but also viable from a humanitarian standpoint. Figure 2-2 represents the building performance levels deemed appropriate by the *NEHRP Guidelines for the Seismic Rehabilitation of Buildings*. It is obvious that collapse prevention and life safety are the most basic requirements of a structure, but in many cases better building performance is a must. For example, if a manufacturing plant or large office building cannot be immediately occupied, literally millions of dollars could be lost due to downtime. Furthermore, hospitals, police stations, fire stations, public works sites, and other civilian entities are vital to the well-being of a society.

Building Performance Levels and Ranges

Performance Level: the intended post-earthquake condition of a building; a well-defined point on a scale measuring how much loss is caused by earthquake damage. In addition to casualties, loss may be in terms of property and operational capability.

Performance Range: a range or band of performance, rather than a discrete level.

Designations of Performance Levels and Ranges: Performance is separated into descriptions of damage of structural and nonstructural systems; structural designations are S-1 through S-5 and nonstructural designations are N-A through N-D.

Building Performance Level: The combination of a Structural Performance Level and a Nonstructural Performance Level to form a complete description of an overall damage level.

Rehabilitation Objective: The combination of a Performance Level or Range with Seismic Demand Criteria.

higher performance
less loss

Operational Level
Backup utility services
maintain functions; very little
damage. (S1+NA)

Immediate Occupancy Level
The building receives a "green
tag" (safe to occupy) inspection
rating; any repairs are minor.
(S1+NB)

Life Safety Level
Structure remains stable and
has significant reserve
capacity; hazardous
nonstructural damage is
controlled. (S3+NC)

Collapse Prevention Level
The building remains standing,
but only barely; any other
damage or loss is acceptable.
(S5+NE)

lower performance
more loss

Figure 2-2: FEMA Building Performance Guidelines [5]

The *Guidelines* have paid particular attention to the overall goal of a building project. While it is most important for a building to stand up and to minimize human injury or death, the *Guidelines* have combined the effects of damage to non-structural aspects. It should be noted that all performance levels are qualitative in nature and take a certain degree of expertise and experience to be of the proper use. Following is a description of the various safety levels ranges outlined in the *Guidelines*:

- **Immediate Occupancy Performance Level (S-1)**

  The status of the building after earthquake has little to no structural damage. The load resisting members retain all of their pre-earthquake capacities.

- **Damage Control Performance Range (S-2)**

  Range of damage states that vary between the pristine state of Immediate Occupancy Performance Level and the moderately damaged Life Safety Performance Level.

- **Life Safety Performance Level (S-3)**

  The building has experience significant damage and structural members have lost a significant amount of load-carrying capacity. However, a safe margin still exists against total collapse, and minimal human injury occurs, particularly no deaths.

- **Limited State Performance Range (S-4)**

  Range of damage states between the Life Safety Performance Level and the Collapse Prevention Performance Level, which can be quite dangerous.

- **Collapse Prevention Performance Level (S-5)**

  Substantial damage has been done to structural system, and building is on the verge of collapse. Yet structural members must still be able to resist gravity load

demands. Building is not safe for reoccupancy and much caution should be taken during repair or destruction processes.

At the Operational Level, notice that a combined rating S1+NA must be obtained (see FEMA Building Performance Guidelines). This means that neither the structure nor the non-structural components, such as HVAC, electrical, and architectural features, can be damaged. This places even more emphasis on the design of the structure, since in reality the motion of a building is controlled first and foremost by its structure. It is the goal of this research to create a methodology that will allow structures to fall in the Immediate Occupancy Level under extreme events. This is a clear enough goal, however one must next ascertain what an "Extreme Event" is.

2.3 Design for Seismic Hazard Levels

The *Guidelines* specify a Basic Safety Objective (BSO), in which a building must satisfy two criteria: (1) the Life Safety Performance Level described above for a moderate earthquake, and (2) the Collapse Prevention Performance Level under a stronger shaking, or more extreme earthquake [4]. FEMA refers to the Basic Safety Earthquake 1 (BSE-1) and Basic Safety Earthquake 2 (BSE-2) to define moderate and extreme events, respectively. A brief explanation of BSE earthquakes will follow.

This philosophy seems to coincide with the typical building codes as well as those of designers and owners historically. Under an earthquake with a high probability of occurrence, a structure should behave elastically and thus no damage will occur. Under a slightly more intense earthquake, the BSE-1, it is most important to have some reserve design capacity, and finally under a high intensity excitation, the BSE-2, the building should simply remain intact. This thesis proposes a more conservative philosophy, in which the building will remain entirely elastic under a BSE-1 earthquake and maintain the Life Safety Level under an extreme event. Such a design level is referred to as an

Enhanced Rehabilitation Objective, meaning that the building performance exceeds that proposed by FEMA for a Basic Safety Objective (BSO). This way of thinking directly coincides with the economic and humanitarian analyses outlined earlier and presented in detail by Wada[2], Huang[2] and Iwata[3] [6].

Table 2.1: Rehabilitation Objectives [5]

		Building Performance Levels			
		Operational Performance Level (1-A)	Immediate Occupancy Performance Level (1-B)	Life Safety Performance Level (3-C)	Collapse Prevention Performance Level (5-E)
Earthquake Hazard Level	50%/50 year	a	b	c	d
	20%/50 year	e	f	g	h
	BSE-1 (10%/50 year)	i	j	k	l
	BSE-2 (2%/50 year)	m	n	o	p

Observe the performance levels associated with the BSO proposed in the *Guidelines* shaded in light gray, compared to the more conservative design objectives proposed in this thesis shaded in dark gray.

2.4 Earthquake Intensity Levels

Hazard level in an earthquake is based on the probability of occurrence in a 50-year period [4] and those levels are used in the FEMA Guidelines and typical earthquake design scenarios. These levels are outlined below:

Table 2.2: Earthquake Return Periods [5]

Probability of Exceedance	Mean Return Period (years)
50%/50 year	72 (round to 75)
10%/50 year	474 (round to 500)
2%/50 year	2475 (round to 2500)

Unlike the existing design methods whereby equivalent static force(s) are applied to the structure, this thesis proposes to perform a time-history analysis with equivalent BSE-1 and BSE-2 earthquakes. In this analysis the Northridge, California 1994 earthquake is used. According to FEMA-355C, this earthquake is approximately representative of the 10%/50 year earthquake with a peak ground acceleration, PGA, of 253.7 in/sec^2 or 6.44 m/sec^2. The study uses a scale factor of 1.03 to achieve the equivalent BSE-1 earthquake, so this analysis will use the original earthquake record as an approximation for the BSE-1. To obtain a BSE-2 earthquake, FEMA scales the earthquake record by 1.29 for a PGA of 357.8 in/sec^2 or 9.08 m/sec^2. This analysis will use a scale factor of 1.5 times the original earthquake magnitude to attain the equivalent BSE-2 earthquake, adding conservatism to the design. The time history data for this earthquake are taken from the United States Geological Survey. Note that the earthquake record for a 50-year return is the original Northridge earthquake scaled down by half. Please refer to Appendix A for earthquakes used by FEMA to represent various earthquake levels.

Northridge Earthquake Scaled to 75 yr Return

(a)

Northridge Earthquake Scaled to 500 yr Return (BSE1)
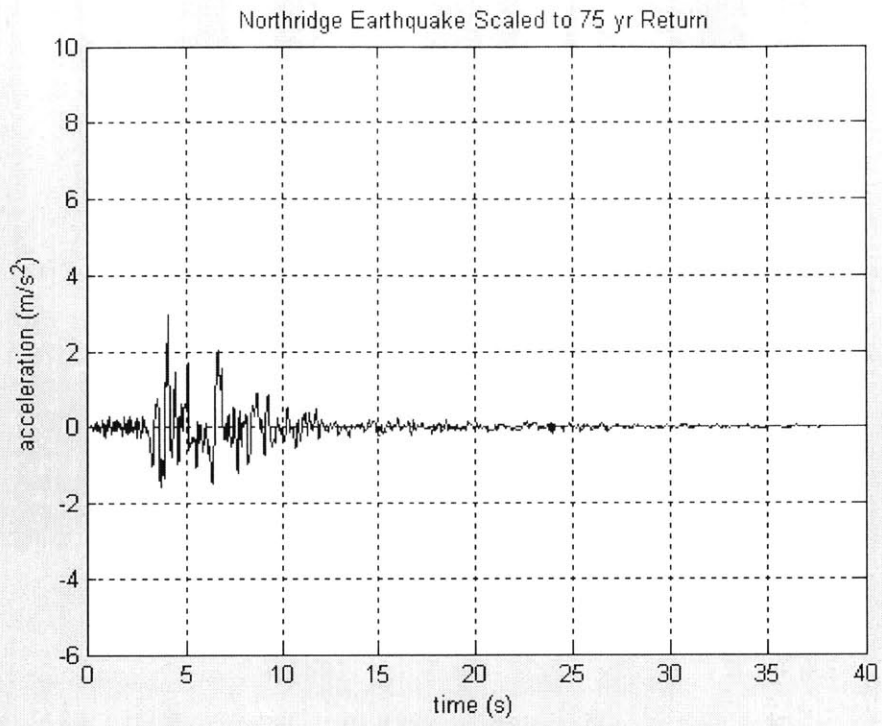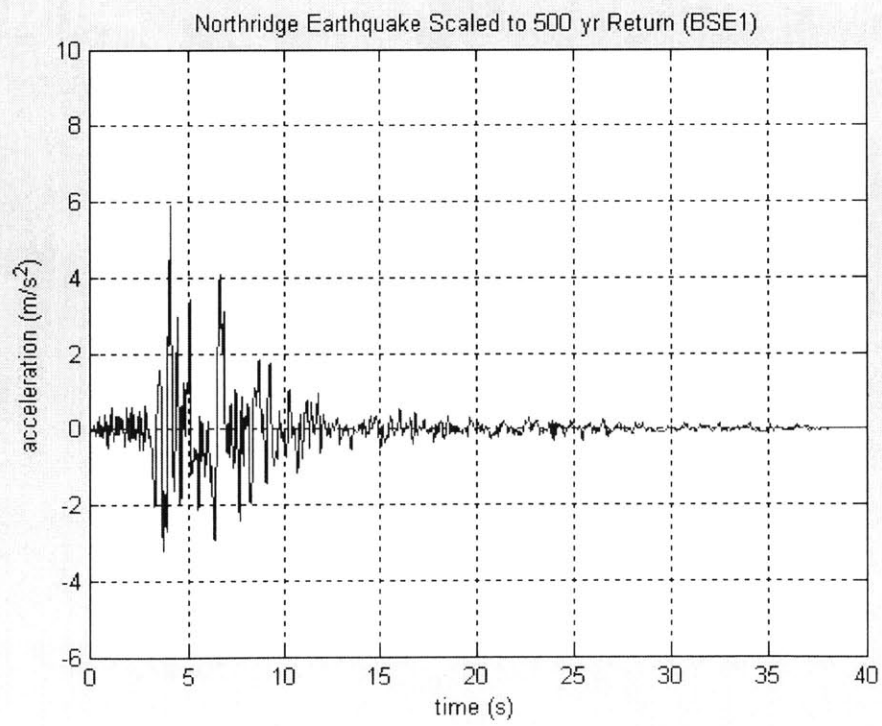
(b)
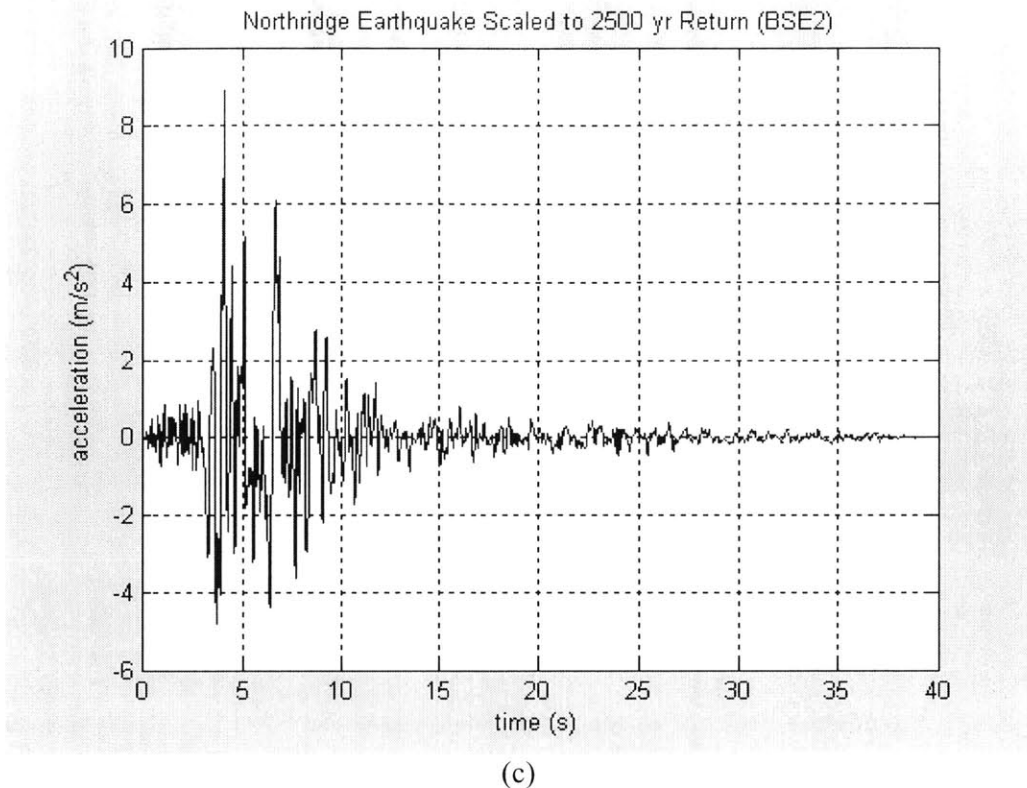
**Figure 2-3: Time History Plots of Northridge, 1994 Earthquake,
Scaled to 75 yr return, BSE-1, and BSE-2**

2.5 Energy Dissipation Methods

During an earthquake event, large amounts of energy are input into the structural system, and this energy must be absorbed in some fashion. The structure must either store or dissipate the energy. In many cases a building has insufficient means of energy dissipation, meaning the energy is stored in the structural members. Stored energy is directly analogous to strain, or deformation, in the members, resulting in severe damage or collapse. Therefore it is necessary in seismic regions to introduce a means for energy dissipation in order to reduce the amount of energy actually stored in the primary structural members. Connor attributes energy dissipation and absorption to several external and internal mechanisms [2]:

- Dissipation due to the viscosity of the material: *viscoelastic materials*.

- Dissipation and absorption caused by the material undergoing cyclic inelastic deformation and ending up with some residual deformation: *hysteretic damping*.

- Dissipation associated with the friction between bodies in contact: *Coulomb damping*.

- Dissipation resulting from interaction of the structure with surrounding environment, through drag force.

Several types of passive damping mechanisms exist, including viscous dampers, friction brace dampers, and hysteretic damper elements. In addition, a base isolation system can be used for seismic design, whereby energy is prevented from being transmitted from the ground motion upward through the structure via an assortment of elastic materials at the base.

Besides the passive damping mechanisms, active control may be pursued. Rather than using a system with fixed properties to absorb and/or dissipate the external energy applied through the earthquake, active control uses external sources of energy to minimize the motion of a structure, and its properties can be dynamically modified according to the loading and system properties. This can be done through a variety of actuators, active prestressing of structural elements, or many other means. See [2] for a more in depth discussion of these methods.

As outlined above, it is the goal of this thesis to present a formal design methodology for the use of hysteretic dampers in seismic design. Before proceeding to the analysis and results of this research, one must gain a fundamental understanding of the properties of hysteretic dampers and the potential associated with using these elements to control motion.

Chapter 3

Hysteretic Dampers

With all the viable energy dissipation mechanisms outlined in the previous chapter, why choose hysteretic dampers? According to Wada et al, the advantages of these devices lie in their low cost, long-term reliability, and lack of dependence on mechanical components [9]. To understand why using hysteretic dampers is an attractive solution for seismic design, one must understand the physical properties of the dampers and the proposed measures for implementation in both design and construction. This section presents this information as background and then reinforces the assertion that hysteretic damping is a practical design solution with a presentation of current design procedures, existing applications, and past experimental results.

3.1 Properties of Hysteretic Dampers

For typical frame structures, i.e. no damping or bracing elements, energy dissipation is achieved through plastic deformation of the flanges of beam-ends [4]. The beam ends are essentially sacrificed to maintain the integrity of the rest of the structure. This can be a poor way to resist earthquakes for two reasons. First, the Northridge Earthquake clearly demonstrated that little energy absorption could be expected from plastic deformation of beam-ends [6]. Once the beam-ends go into plastic deformation large deformation of the entire frame results, thus defeating the purpose of deflection controlled design. Secondly, the beam-ends need to be inspected after an earthquake and repaired and/or replaced if damaged. Access is a key issue, as most of the structure will be concealed by architectural components, and repairing the flanges could be highly detrimental to the strength of the structure during the time of repair. Replacing the flanges cannot be done, meaning the structure will require some type of retrofit or will be rendered useless.

The theory of using hysteretic dampers is analogous to the design of beam-ends to yield during earthquake excitation. Input energy is absorbed essentially through the yielding of the hysteretic damper, while the rest of the structure would ideally remain intact and experience only elastic deformation. To ensure that the energy is in fact being absorbed by axial yielding in the hysteretic damper, the yield force level in the damper must be significantly lower than the rest of the structure. This approach takes into account the two fundamental flaws of pure framed structures described in the previous paragraph. If the damper yields, the rest of the structure remains intact with its elastic stiffness, thus reducing the amount of motion induced by an earthquake. Since the damper is effectively an addition to the typical primary structure, permanent damage to the damper has no effect on the structural integrity. To use the nomenclature of Wada, Huang, and Iwata, the damper is used as a 'sacrificial' element. Ideally the damaged brace could be replaced easily in terms of ease-of-access for workers and economics.

During an earthquake, structural elements displace in two directions, since the loading is cyclic in nature. Also, a typical bracing scheme places the brace at 45^0 in a frame consisting of columns and beams. Because of the cyclic motion of the structure, the brace will go into tension and compression. Thus, the hysteretic damper must be designed so as to provide identical tensile and compressive properties. Figure 3-1 illustrates such a bracing element, which consists of a yielding core element and a stiff jacket with little to no friction between the two elements. Such a member is called an unbonded brace. The "unbonding material" allows the yielding core element to move independently of the jacket, while the jacket provides the cross sectional moment of inertia to resist buckling under compression [2]. The brace behaves elastically with an inherent stiffness when the applied force is lower than the material yield force value. In the idealized case, once this force is reached the brace will continue to displace without an increase in applied force, which is based on the elastic-perfectly plastic model. Once the force is reversed the brace provides the same elastic stiffness until the yield force is reached in compression. This process continues under cyclic loading and is known as a hysteresis loop. See Figure 3-2.

encasing
mortar

yielding steel core

"unbonding" material between
steel core and mortar

steel tube
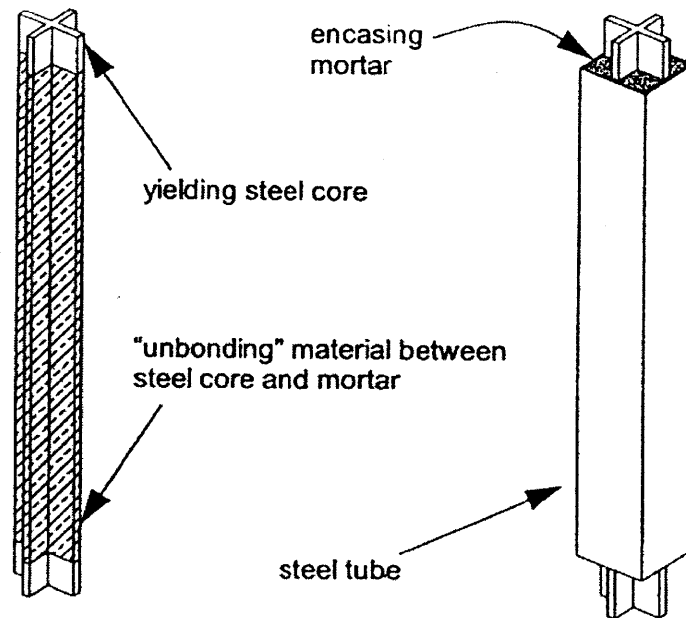
Figure 3-1: Hysteretic Damper (Unbonded Brace) [9]

tension

**Yield
Force**

Stiffness

displacement

typical
buckling
brace

**Yield
Displacement**

unbonded
brace

compression

Axial force-displacement behavior
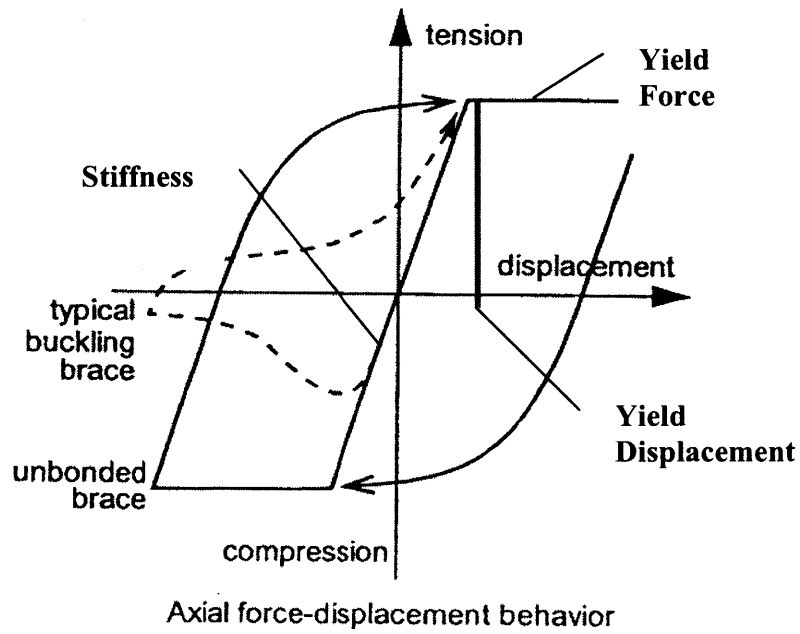
Figure 3-2: Hysteretic Behavior of Unbonded Brace [9]

23

3.2 Design Procedures

The key structural parameters of the unbonded brace are strength, stiffness, and yield displacement (ductility) [9]. By varying these parameters, the designer can obtain the necessary force-displacement relationship of the lateral motion-resisting elements for the particular design application. On a system level, one of the most important design parameters is the relationship between the frame and damper properties. Yamaguchi[4] and El-Abd[8] introduce a constitutive model of a frame with hysteretic damper, which is vital to the analysis done in this research. The initial stiffness, the yield shear force and corresponding yield displacement for the frame and the damper are K_F, K_D, Q_F, Q_V and Δ_F, Δ_F respectively [11]. It should be noted that the hysteretic damper not only provides the damping qualities associated with material yielding but also increases the lateral stiffness of the structure, which is quite beneficial when attempting to control structural motion.
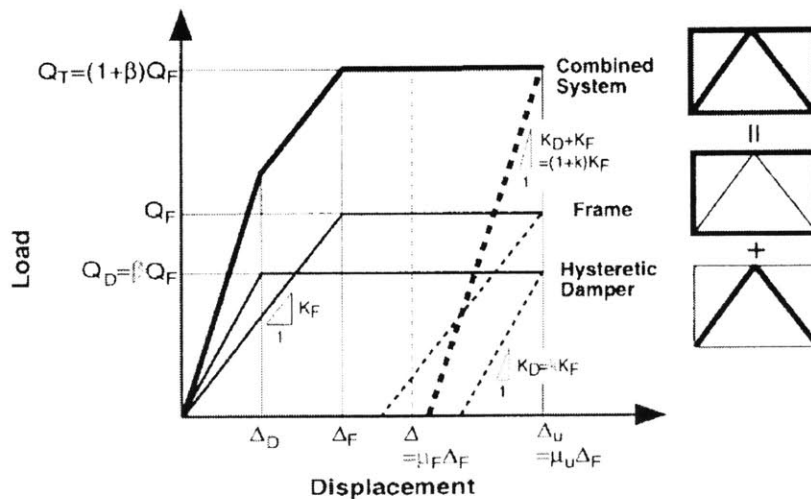
Figure 3-3: Constitutive Model of Frame with Hysteretic Damper [11]

Yamaguchi and El-Abd have also developed an energy and performance based prediction of damper efficiency. This prediction is based on the correlation of certain earthquake

---

input parameters, including the effective duration of the earthquake Δt_{eff}, dominant response period T_D, and equivalent velocity, $V_{e,sdof}$. Based on the damper properties shown in Figure 3-3 and the mass M of the building, the damper efficiency is quantified as:

$$\alpha \equiv \frac{MV_e^2 T_D}{\Delta t_{eff}^E \sum_{i=1}^N Q_F^i \Delta_F^i}$$

This approach is largely based on experimental data for the determination of correlations between response parameters and earthquake characteristics. It is shown that the damper performance is highly dependent not only on frequency domain parameters (maximum energy input and dominant earthquake period) but also on earthquake time-dependent parameters such as effective duration.

3.3 Existing Applications

As of August 2001, more than 160 buildings in Japan have employed the use of hysteretic dampers and it is beginning to gain popularity in the United States. Nippon Steel Corporation, the Japanese producers of low-yield strength steel used in the hysteretic dampers in Japan, are entering the domestic market, particularly in California and the West Coast [4]. The Wallace F. Bennett Federal Building in Salt Lake City, Utah was retrofitted with unbonded braces in order to meet stricter current seismic codes. Table 3-1 below lists several mid to high-rise buildings constructed in the late 1990s. Outlined below are two particularly interesting design cases.

3.3.1 DoCoMo Tokyo Building

This 50 story, 240 meter mixed-use employs the use of both a viscous damping system and a steel frame structure with steel braces. The bottom 27 stories are used for office and are controlled via 76 viscous damping walls, while the top 23 stories, used for mobile

communication, are damped through the use of braces like that described in this thesis. This design is significant for two reasons: 1) it employs both hysteretic and viscous dampers, which coincides with the analysis method used in this research and 2) the primary steel structure is designed within the elastic region even under the second level of earthquake (approximately BSE-1) [6].
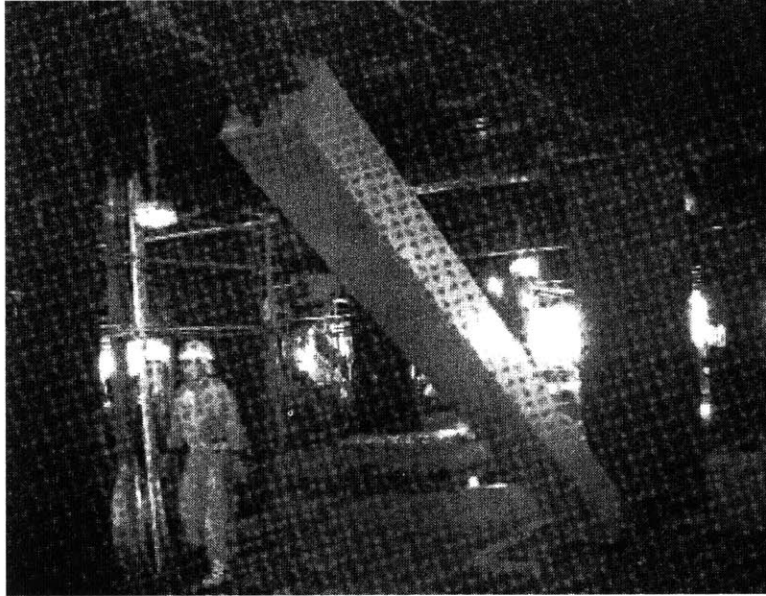
Figure 3-4: Existing Unbonded Brace Scheme [2]

3.3.2 Central Government Building

In the same way that the DoCoMo Tokyo Building is designed for the primary structure to remain elastic under a second level earthquake, the Central Government Building achieves this goal. Also, the engineers used a combination of hysteretic dampers and viscous dampers to achieve the design goals. As a design parameter it is assumed that the yield shear force level of the hysteretic dampers is equal to 5% of the total building weight [6]. The research in this thesis hopes to provide a more analytical approach to forming such a design parameter.

It should be noted that most of these buildings are moderately tall, approximately 100 meters in height. This suggests, as does [2], that hysteretic dampers are most effective for the design of mid-rise buildings. This provides a basis for the analytical model used in this research, which depicts a 10-story building.

Table 3.1: Buildings in Japan designed using hysteretic dampers [6]

Year	Project's name	Location	Usage	Height (m)	Structure type	Dampers	Ductility ratio
1995.6	International Congress	Osaka	Congress	104	S_F	HD_B	0.95
1995.7	Todai Hospital	Tokyo	Hospital	82	S_F	VD_S	0.93
1995.7	Tohokudai Hospital	Sendai	Hospital	80	S_F	VD_S	0.97
1995.8	Central Government	Tokyo	Office	100	S_F	HD_B + VD_S	0.78
1995.10	Harumi 1 Chome	Tokyo	Office, Shop	175	S_F	HD_B	0.88
1996.2	Toranomon 2 Chome	Tokyo	Office, Shop	94	S_F	VD_S	0.94
1996.3	Passage Garden	Tokyo	Office	61	S_F	HD_B	0.88
1996.4	Shiba 3 Chome	Tokyo	Office	152	S_F	HD_B	0.97
1996.6	Art Hotel	Sapporo	Hotel	96	S_F	HD_BD	0.85
1996.8	Kanto Post Office	Saitama	Office	130	S_F	VD_S	0.87
1996.10	Nakano Urban	Tokyo	Office, Shop	96	S_F	VD_S	0.68
1997.7	DoCoMo Tokyo	Tokyo	Communication, etc.	240	S_F	VD_S	0.79
1997.10	Minato Future	Yokohama	Hotel, Shop, Office	99	S_F	HD_BD	0.98
1997.11	Nishiguchi Shintoshin	Yamagata	Office, Hotel, etc.	110	S_F	HD_B	1.00
1998.2	DoCoMo Nagano	Nagano	Communication	75	S_F	VD_S	0.89
1998.4	East Osaka City	East Osaka	Office	120	S_F	HD_S	1.00
1998.5	Kouraku Mori	Tokyo	Office, Shop	82	S_F	HD_B	1.00
1998.7	Harumi 1 Chome	Tokyo	Office, Shop, etc.	88	RC_F	HD_B	1.00
1998.11	Adago 2 Chome	Tokyo	Office, Shop	187	S_F	VD_B	0.71
1998.11	Gunyama Station	Fukushima	Shop, School, etc.	128	S_F	HD_B + VD_S	0.98

3.4 Past Results

Hysteretic dampers have been studied in two different ways: 1) on a material level, or in terms of individual damper behavior and 2) on a system level, or overall building analysis. Following is an illustration of experimental results and analytical models from past research.

3.4.1 Material Properties

There has been extensive testing done on unbonded braces because of the potential advantages described at the beginning of this chapter. One such test, performed by Clark,

Aiken, Ko, Kasai, and Kimura in conjunction with University of California-Davis coincides with idealized hysteresis loop shown in Figure 3-2. In these tests an incremental equivalent interstory drift time history, computed from the UC Davis Plant & Environmental Sciences Replacement facility, was applied to an unbonded brace. This protocol was derived from that used in the Phase 2 Sac Steel Project [9]. The following figure illustrates the loading history applied to the test brace.
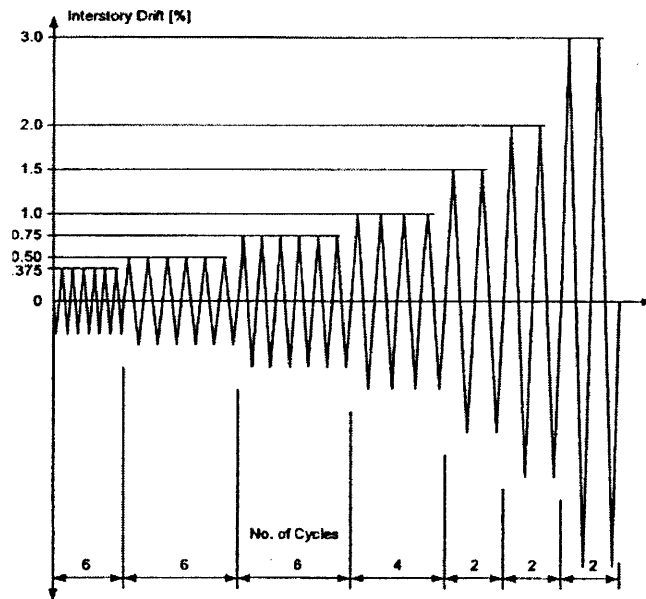
Figure 3-5: SAC Basic Loading History [9]

For a test specimen with a core area of 4.5 in^2, a yield force of 270 kips, and a rectangular shaped yielding section [9], the following force-displacement relationship was found under the SAC Basic Loading History.

Observe the nearly ideal hysteretic response of the test specimen in both tension and compression. When compared to the ideal case (see Figure 3-2), the shape is nearly identical. This is not a trivial result given the fact that most analytical models, in particular the model used in this analysis, assume elastic-perfectly plastic behavior for the hysteretic elements. Three different test specimens were tested under two different loading histories, and the results were astonishingly consistent. While the yield force

level, elastic stiffness, and maximum displacement differed for each test code, this nearly elastic-perfectly plastic hysteresis loop ensued for each case. Refer to [9] for detailed results of these findings.
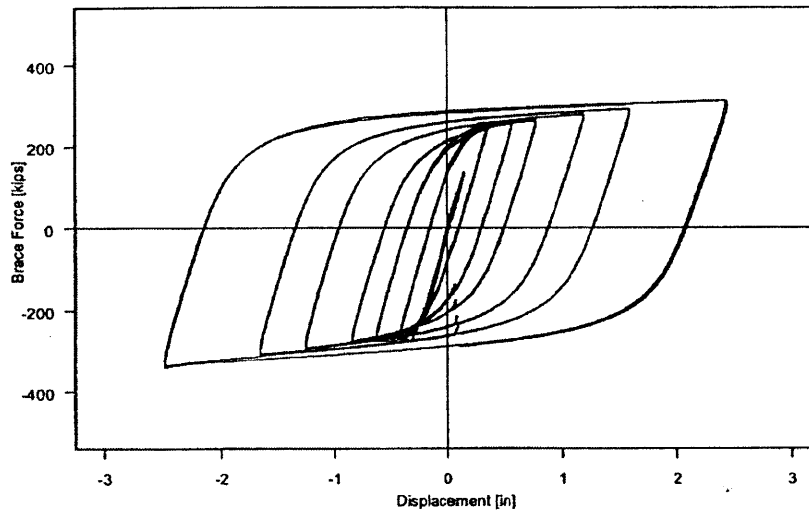
Figure 3-6: Hysteretic Response of Unbonded Brace Specimen

3.4.2 Building Analyses

A study by Wada, Huang, and Iwata was designed to experimentally compare the qualities of a typical beam/column frame system with that of a braced system. A series of static cyclic loading and dynamic loading tests were carried out on a Moment Resisting Frame and a slender Moment Resisting Frame with an unbonded brace. It was confirmed from these experimental studies that the DCS (the braced scheme) is much better than the conventional steel structure in the energy dissipation capacity [6]. Two major findings occurred from this research. First, the unbraced frame received tremendous amounts of plastic deformation under the loading, while the primary structure of the brace frame remained nearly elastic even under a considerable drift angle of 1/50. Secondly, the weight of the primary structure was reduced significantly. In two test cases, one using mild steel and the other using high strength steel, the weight of the

primary structure was reduced by over 30%. This could result in noteworthy cost savings both because of the reduction in the amount of steel in the frame itself but also in the size of the structure below, since structural dead loads would in turn be reduced.

An analytical model developed in [9] coincides directly with these experimental results. This model consisted of a typical three-story frame redesigned with unbonded braces and used the equivalent static lateral force provisions from the UBC. It is shown that the total weight of the steel (including unbonded braces) in the unbonded brace frame is only 0.51 times that of the moment resisting frame. Furthermore, this design would require substantially fewer rigid connections than a moment resisting frame, so it would be expected to be less expensive to build. Where the W14x68 beams are used in Figure 3-7, a W33x118 beam would be necessary for a moment resisting frame.
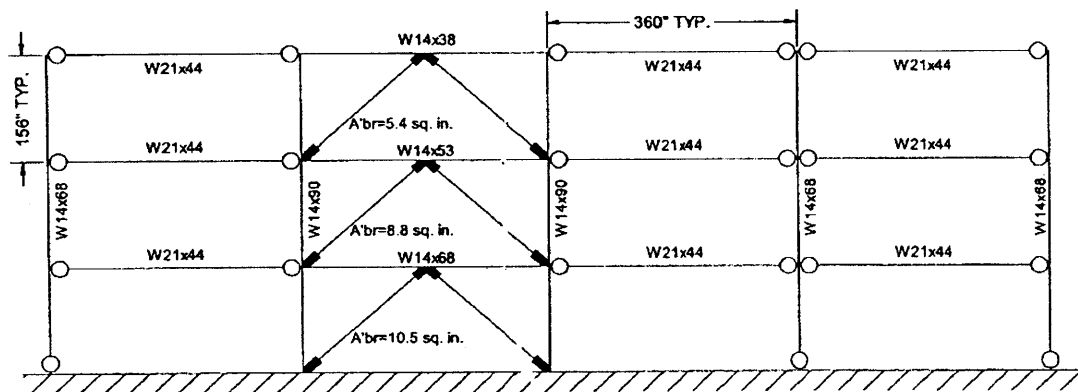
Figure 3-7: Three-Story Moment Frame Redesigned as a Braced Frame [9]

A further application of this study evaluates the performance of the unbonded brace frame to an eccentrically braced and concentrically braced frame. While all of the braced frames perform better under earthquake loads than a moment resisting frame, the unbonded brace structural system has the lowest roof displacement and the highest base shear to weight ratio. Also, the unbonded brace frame is the only system to achieve the life safety performance level outlined in the *Guidelines*, while the other two systems achieve only collapse prevention performance level [9]. These studies suggest the

growing potential and need both for further research into hysteretic damper design for civil structures and the increased implementation of this design philosophy, particularly in domestic projects.

Chapter 4

Present Design and Experimental Work

One of simplest means of designing hysteretic dampers is to calibrate the energy dissipation capacity. The energy dissipated by the mechanism is represented by the area within the hysteresis curve shown in Figure 3-2 [4]. Thus, by tweaking the yield force level, F_y, or increasing the ductility ratio, which relates the maximum displacement of the brace to the yield displacement, the effective damping can be varied. A highly ductile material with a sizeable yield force level will dissipate large amounts of energy. In order to be effective at high levels of excitation, like a BSE-1 or BSE-2 earthquake, the damper must have sufficiently high yield force and ductility ratio. Effectively the damper acts as a stiffening element during the majority of its life and only acts as a damper in rare seismic events.

Nippon Steel Corporation, in Japan, has been a major developer of this concept and has a large hold in the market of developing hysteretic dampers for civil structures. Virtually all of the buildings with unbonded braces outlined in Table 3-1 use Nippon Steel products. Over the history of its development of unbonded braces, Nippon has increasingly pursued stiffening elements, i.e. high yield force level, versus energy dissipation characteristics, or lower yield force level. This design philosophy has resulted in very robust braces that are inexpensive but very heavy. The weight causes construction issues, as machinery is generally required for installation, making these braces a somewhat unreasonable alternative for the retrofitting of existing structures. Also, in scenarios where energy dissipation is more important than increasing stiffness, this kind of brace will not be necessary. Shorter buildings tend to have smaller periods than their taller counterparts and are thus highly susceptible to most earthquakes due to resonance, because of the frequency content typical of most earthquakes on record. Thus, increased stiffness is needed for buildings under ten stories that reside in highly seismic

zones. However, taller buildings could be an appropriate application for dampers with lower yield force levels due to the need for energy dissipation, or damping.

Kazak Composites Incorporated (KCI), Woburn, MA, has adopted this philosophy in its approach to developing practical civil engineering materials. The initial hysteretic design concept proposed by KCI was to produce a light, low yield force brace with the aim of being used in retrofit applications. Preliminary analysis suggested yield levels on the order of 100 kip. However, through finite-element analyses of a 3-story building it was found, as suggested above, that energy absorption in this case is less useful than added stiffness. Yield force levels of 300 kip-500 kip would be required-which would necessitate heavy and perhaps expensive materials-a major departure from the original philosophy of the company [8]. Another noteworthy observation made in the KCI study is an outline of the tradeoffs associated with unbonded brace design: balancing stiffness versus damping is a difficult task, mass production of dampers must cater to a variety of building types and excitations, and cost tradeoffs versus other types of braces and/or dampers must be considered. This thesis proposes to provide a general methodology for tackling the first problem, calibrating the proper yield force distribution throughout a building.

As a supplement to the theoretical modeling done in this research, several tests were performed with Pavel Bystricky[5] and Todd Radford[6]. KCI is currently developing a proprietary unbonded bracing scheme, which is intended to for the design goals originally proposed by Kazak Composites in 2000; producing lighter braces that require little construction/installation effort, yet provide an optimal damping solution [4]. The testing protocol used for this research is consistent with the SAC Basic Loading History used in the UC-Davis study outlined earlier. Following is an outline of the loading history used at MIT.

---

[5] Kazak Composites Incorporated
[6] Massachusetts Institute of Technology

The force-deformation relationship shown in Figure 4-1 illustrates a nearly ideal hysteresis loop. Under large deformations, the elastic-perfectly plastic model holds true, with a yield force level of approximately 48 kip and an elastic stiffness of 335 kip/in.

Table 4.1: Loading History

Cycles	Displacement (in)
6	0.06
6	0.08
6	0.12
4	0.16
2	0.24
2	0.32
2	0.48

Notice, however, the increase in axial force capacity under large compressive deformations. Current speculation indicates that this phenomenon could be the result of two things. One conjecture is that the confinement provided by the anti-buckling sleeve restricts the Poisson's effect of the yielding material; this biaxial behavior results in an increase in axial strength. Secondly, the yielding material is actually buckling, however the confinement again causes an increased stress state. There could be several other explanations, and this trend must be explored further. It should also be noted that this increase in stiffness could actually be beneficial to a structure in practice, given the necessity for stiffness in a motion based design approach. However, this must be included in the design and analytical tools.

Past design examples and experimentation, along with current research, provide an important basis for this proposal. Not only is it important to understand current design trends when trying to develop a new methodology, it is necessary to have a fundamental understanding of the properties of the devices used for this design approach. The last two chapters have illustrated that using hysteretic dampers, or unbonded braces, for seismic design is both feasible and full of potential. Furthermore, this gives insight into the limits and promise of the devices themselves. When designing a structure in general or more specifically when trying to predict the optimal stiffness and yield force distribution

throughout a building, it is important to know what is conceivable given current industry developments.
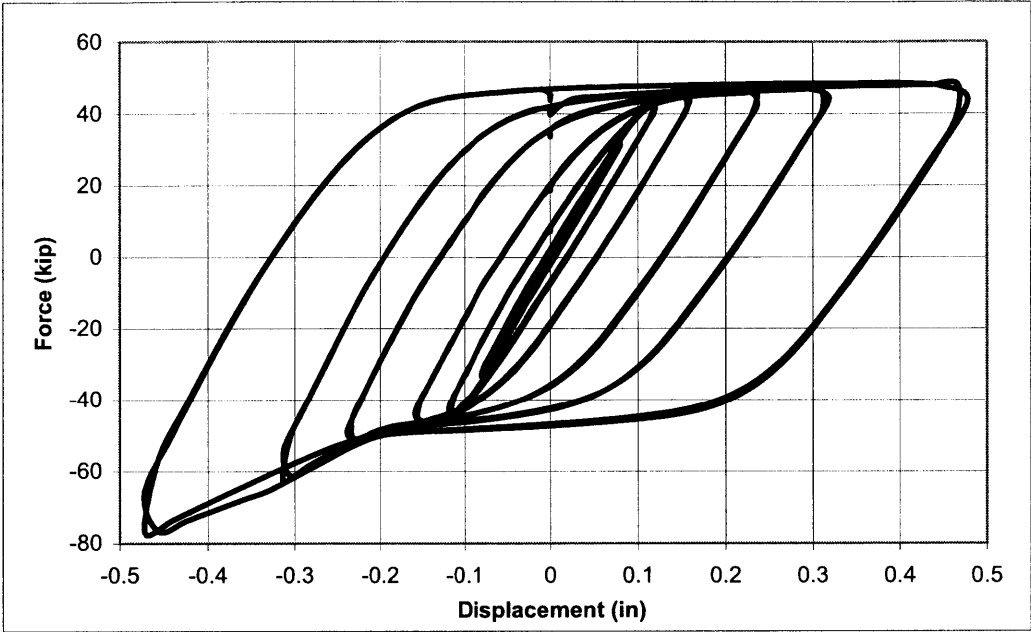
Figure 4-1: Hysteresis Loop for KCI Prototype

Chapter 5

Analysis

The object of this research is to establish a distribution of structural stiffness for a building under an extreme event in order to achieve a specified displacement profile, the essence of the motion based design approach proposed by Connor. In the same way that the deformation of a spring under a certain load depends directly on the stiffness of the spring, so does the displacement of a building depend on its inherent stiffness. The stiffer the structure, the smaller the displacement under a given load. Obviously an infinitely stiff building would result in zero relative displacement (the relationship between the building and the foundation on which it rests) during an earthquake. This seems to be the clear solution, however it is detrimental for two reasons. Aside from the impossibility of developing an infinitely stiff building, the costs of doing so would theoretically be enormous. Also, if a building were infinitely stiff, it would move exactly in-phase with the ground motion. The occupants, whether they be human or machine, would then be very uncomfortable and enormous shear forces result. Thus, the calibration of stiffness becomes a very difficult process. The engineer must select a set of parameters that he or she feels best represents the needs of the project. These parameters will be explored in the next chapter. The optimal solution is not easily predicted; therefore a series of iterations must be made to converge on the desired results. Before proceeding to the computer algorithm used in this analysis, one must first understand the basic physics used to develop the model.

5.1 Governing Equations for a Multi-story Building

The theory used in this analysis is merely an extension of basic linear spring theory. The single degree of freedom, spring-mass-damper model is shown in Figure 5-1. In the simplest case where the force is applied statically:

$$P = Ku \qquad (5.01)$$

In the dynamic case, another term associated with the inertia of the mass (known as the D'Alembert Force, or inertial force) is added.

$$P = m\ddot{u} + ku \qquad (5.02)$$

Finally, if the system has some type of viscous damping or an equivalent, which is proportional to the velocity of the mass, the equilibrium equation becomes:

$$P = m\ddot{u} + c\dot{u} + ku \qquad (5.03)$$
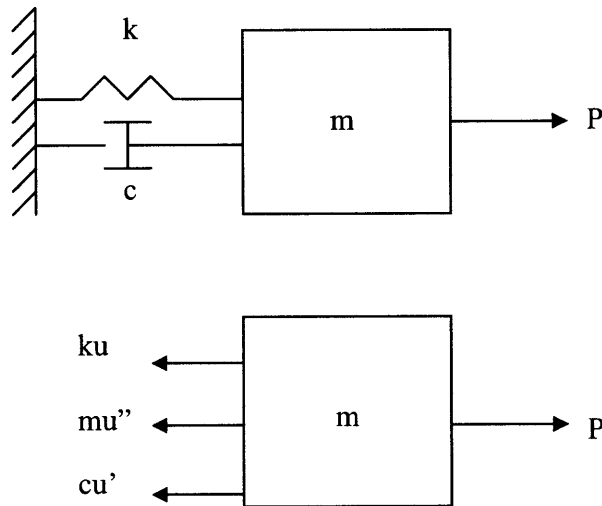
Figure 5-1: Spring Mass Damper Model and its Free-Body Diagram

To extend this approach, the mass of each story is lumped into a discrete volume, and the structural elements between each story act as an equivalent spring. Assuming the structural has either inherent damping or a series of additional dampers, the equilibrium equation Eq. (5.03) still holds true. The multi-degree of freedom system, or shear beam model, requires the use of matrix algebra. The formulation follows in the same way, where each mass has two spring and damper forces, respectively, from the adjacent

structural members both above and below the floor. The equilibrium equation, assuming no damping, then becomes:

$$p_i = m_i \ddot{u}_i + V_i - V_{i+1}$$ (5.04)

Where V is the shear force (equivalent to a spring force) due to the displacement of the masses relative to one another.

$$V_j = k_j (u_j - u_{j-1})$$ (5.05)

Substituting into Eq. (5.04) results in:

$$p_i = m_i \ddot{u}_i - k_i u_{i-1} + (k_i + k_{i+1}) u_i - k_{i+1} u_{i+1}$$ (5.06)

Consolidating this equation into matrix notation

$$\overline{P} = \overline{M\ddot{U}} + \overline{KU}$$ (5.07)

Where the matrices for mass and stiffness are represented by the following [2]

$$M = \begin{bmatrix} m_1 & & & & \\ & m_2 & & & \\ & & \cdot & & \\ & & & \cdot & \\ & & & & \cdot \\ & & & & & m_n \end{bmatrix}$$

$$K = \begin{bmatrix} k_1 + k_2 & -k_2 & 0 & \ldots & 0 & 0 & 0 \\ -k_2 & k_2 + k_3 & -k_3 & \ldots & 0 & 0 & 0 \\ \cdot & \cdot & \cdot \cdot & & \cdot & \cdot & \cdot \\ \cdot & \cdot & \cdot \cdot & & \cdot & \cdot & \cdot \\ \cdot & \cdot & \cdot & \cdot & \cdot & \cdot & \cdot \\ 0 & 0 & 0 & \ldots & -k_{n-1} & k_{n-1} + k_n & -k_n \\ 0 & 0 & 0 & \ldots & 0 & -k_n & k_n \end{bmatrix}$$

The damping matrix is assembled in a similar way to that of stiffness and yields

$$\bar{P} = \overline{M\ddot{U}} + \overline{C\dot{U}} + \overline{KU} \tag{5.08}$$
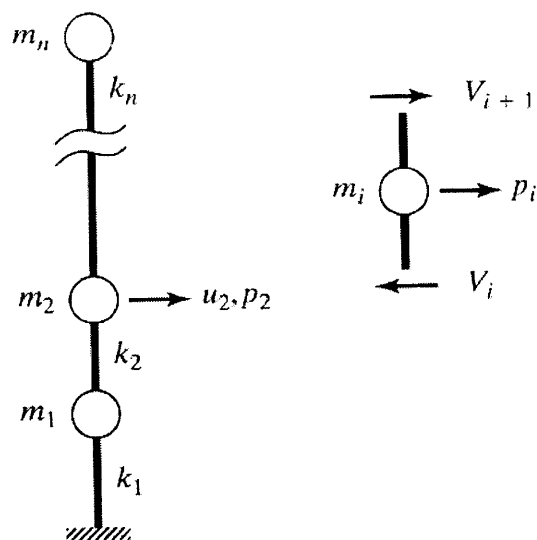
Figure 5-2: General Shear Beam Model [2]

For earthquake analysis, the externally applied force on each element is due to the ground motion, including displacement, velocity, and acceleration. Eq. (5.08) can be manipulated in terms of seismic acceleration and is expressed as:

$$p_i = -m_i a_g \tag{5.09}$$

This development was used throughout the analysis to calculate deformations and to calibrate the optimal stiffness and yield force distribution in the braces.

5.2 Design Strategy

This design strategy proposes a more conservative approach in terms of the seismic response of an earthquake. According to the parameters proposed by FEMA, which are

outlined in Chapter 2, a structure consisting of Braced Steel Frames can have 0.5% transient and negligible permanent drift for BSE-1 to satisfy the Immediate Occupancy Performance Level and 2% transient or permanent drift for BSE-2 to satisfy the Collapse Prevention Performance Level [4]. It is now proposed that the structure satisfy the Immediate Occupancy Performance Level for BSE-1 and *Life Safety Performance Range* (S-3) for BSE-2. This essentially limits the amount of allowable plastic deformation in structural members under an extreme event. As in the *Guidelines* recommendations, the structure should remain elastic, or have negligible permanent deformation, under the 75-year return earthquake. However, this strategy seeks to reduce the amount of plastic deformation in the load-bearing structural members under an extreme event. Therefore, this analysis assumes allowable transient drift of 0.5% under BSE-1 and 1% transient or permanent drift under BSE-2. In Chapter 3 it was stated that the primary structure with an unbonded brace scheme could remain elastic under a drift angle of 1/50, meaning the building could experience 2% transient drift. Thus, a constraint of 1% drift is reasonable for achieving Life Safety Performance Level.

A second departure from current design standards is to perform dynamic analyses as opposed to equivalent static seismic forces, as mentioned earlier. Unless otherwise noted, the 1994 Northridge earthquake is used in the analysis, however several earthquakes could be used in conjunction with Northridge to verify results. While this approach is obviously more accurate than using static equivalent forces, it does have one obvious disadvantage. In areas without a comprehensive seismic history, realistic earthquakes do not exist. Therefore, it becomes difficult to find the proper representative earthquake for analysis. However, when designing in highly seismic areas where extensive geological surveys exist, as is the case on the West Coast and in Japan, this approach is not only practical but necessary.

Using the "sacrificial" element philosophy proposed earlier, the structure is essentially broken into two parts. The primary structure functions as the basic load-bearing system for the building, while the secondary structure is used most fundamentally for seismic or

lateral load resistance. The ultimate goal of this tactic is to preserve the primary load-bearing members, even under extreme events, thus meeting the Life Safety Performance Level. Under said extreme event, the secondary structure yields, resulting in the energy dissipation associated with yielding elements. In order to calibrate the necessary stiffness and yield force values throughout the height of the building, it is assumed that both elements, the primary and secondary structure, remain elastic under BSE-1 while only the *secondary structure* yields under BSE-2. Hence the idea of sacrificial elements: the unbonded braces could easily be replaced, while the integrity of the overall building remains intact.
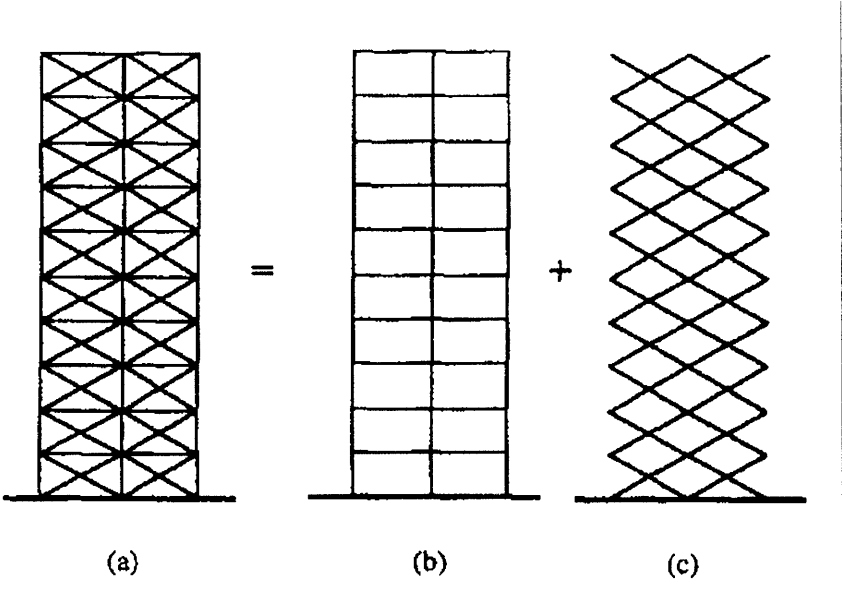
Figure 5-4: Illustration of (a) Overall Structure (b) Primary Structure and (c) Secondary Structure [3]

Furthermore, it is vital to determine the interaction between the primary and secondary structures. The following questions must be asked: how much of the necessary stiffness should be allocated to the primary structure relative to the secondary structure, and how much of the shear force applied to the building be allocated to the primary and secondary structures? To the knowledge of the author this has not been calculated analytically, and so this thesis provides a numerical method for calibrating stiffness and shear force distributions.

41

5.3 Numerical Calibration Method

The model is based on an iterative procedure in which an initial guess at the stiffness distribution and yield force level is required. This is somewhat empirical, however with enough iterations the optimal distribution can be found. It should be noted that a fairly accurate first guess is important, since the program takes computational power, and a reduction in the number of iterations will result in decreasing computational time and cost. The program, written in MATLAB, requires the specification of several parameters. Since it has the ability to analyze any multi-degree of freedom system, it is first necessary to specify the number of floors in the building and the mass of each floor. For this analysis, a 10-story building is used, which is consistent with the size of buildings typically designed with hysteretic dampers [6]. Next, one must specify the percentage of stiffness and shear taken by the braces relative to the overall structural system. For example, if 25% of stiffness is allocated to the braces, then 75% must be taken by the primary structure. Finally, the allowable elastic drift of the building must be specified. According to *Guidelines* specifications of 0.5% from above and for a 4-meter interstory height, the allowable drift is 0.02 meters. In addition to these specifications, an initial guess at the stiffness distribution and yield force values must be made. Based on prior experience and the description in [2], most buildings require a parabolic stiffness distribution in order to maintain quasi-linear deformations.

These initial values are used in conjunction with the theory presented in Section 5.1. With a given externally applied force-in this case the earthquake-and the initial stiffness values, the motion of the structure can be calculated. If the calculated displacement is greater than the specified allowable displacement, the stiffness needs to be increased. Conversely, if the deformation is less than the allowable design value, the structure is over-designed and the stiffness needs to be reduced. In the same way, the shear yielding force is calculated by setting the value equal to the shear force experienced under BSE-1. Therefore, elastic response is ensured. Once the stiffness and yield force values are calibrated for BSE-1, the structure is hit with the extreme event and the response is

analyzed. In this case, the stiffness and yield force distribution are not recalibrated but are based on the values used to remain elastic under the 75-year return earthquake. This algorithm is illustrated schematically in Figure 5-5.

It is most important to be able to easily change the parameters that control stiffness and yield force distribution in a building, specifically the percentage taken by primary structural members versus secondary members. An algorithm originally developed by Connor assumes the lateral force resisting system is entirely the secondary system.

In the early developments of the model, the calibrated stiffness and shear force are taken entirely by the secondary structure. This model is both unrealistic and detrimental to the integrity of the structure. Any frame structural system, particularly a Moment Resistant Frame, has at least some minimal lateral stiffness. In fact, these structures can have significant stiffness, as experiments have shown [6,9]. Therefore assuming no primary stiffness is not realistic. Also, assuming the unbonded braces provide the only lateral support can have quite adverse effects on the response of the building for an extreme seismic event. The braces are calibrated to remain elastic for BSE-1, but for BSE-2 the braces go into yielding and thus lose a considerable amount of stiffness. Yielding of the elements can result in relatively large deformations, which is detrimental to the integrity of the building, and is again not viable. Thus an important addition to the model is the ability to allocate a designated amount of stiffness and shear force to the braces and primary structure. It is equally important to have the ability to do this in a quick fashion, since a parametric study requires several test runs.
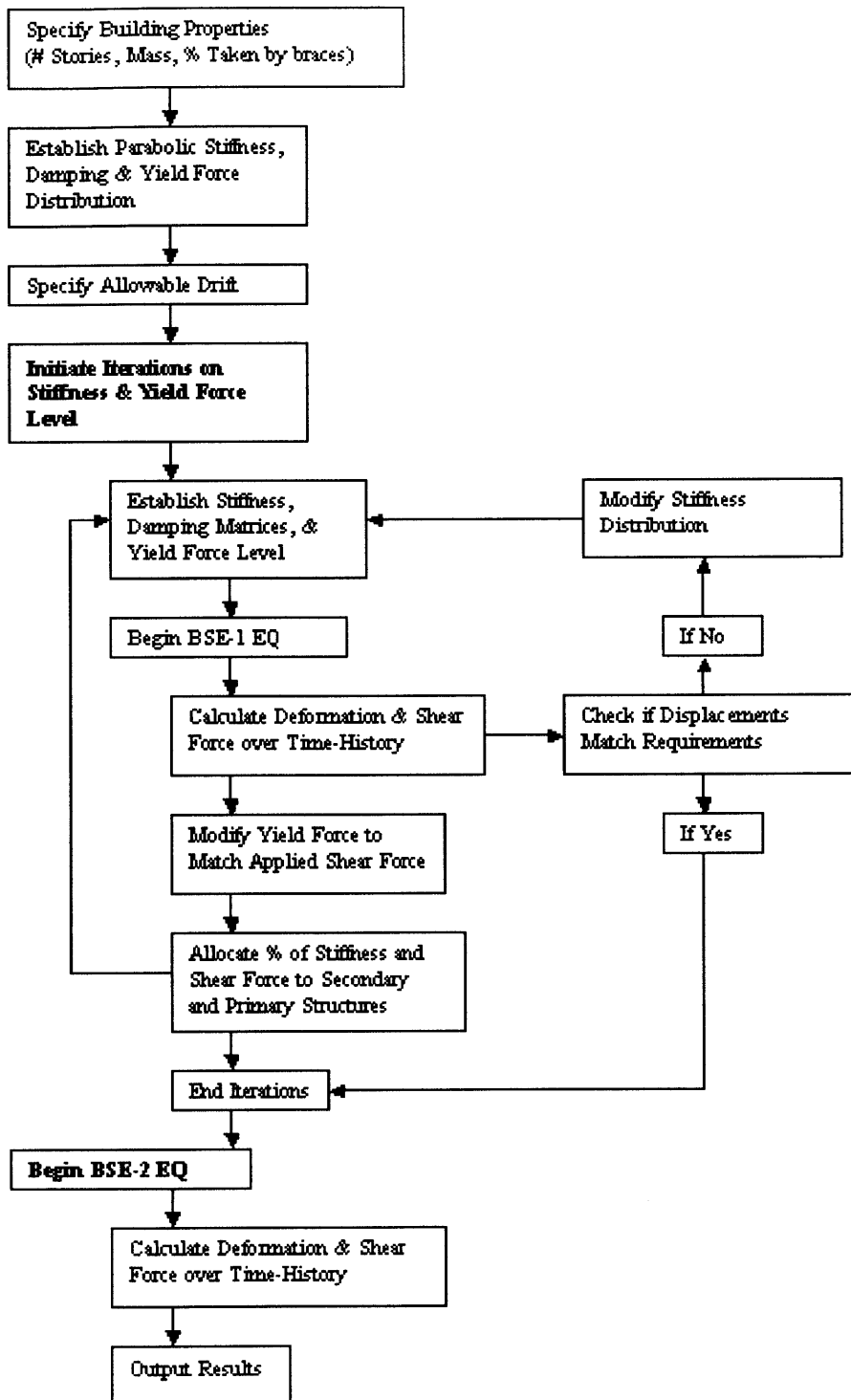
Figure 5-5: MATLAB Algorithm

Chapter 6

Results

With a sufficient understanding of the theory of using hysteretic dampers in buildings; past results in design, analysis, and experimentation; material properties and behavior of unbonded braces; and analysis methods used for this thesis, it is now logical to explore the results of the analysis and draw the subsequent conclusions. The results of this study are broken down into three subtopics: optimal structural properties required to meet the design standard presented earlier, feasibility studies for the practical application of the results obtained, and a cost analysis.

6.1 Optimal Structural Properties

6.1.1 Introduction to Structural Parameters

The structural properties most important to analysis are the stiffness distribution through the building, both for primary and secondary structure; the yield force level of the braces and the horizontal force applied to the primary structure; the drift distribution of the building, both for BSE-1 and BSE-2; and the ductility demand distribution through the structure. Upon the refinement of the algorithm described in the previous chapter a variety of simulations were performed with various brace/primary stiffness and shear force ratios. This parametric study hopes to illustrate the optimal design solution for a typical 10-story building under the Northridge earthquake and its scaled equivalent. As a first conjecture, it is assumed that the optimal allocation of stiffness to the brace is 25% and the same for shear force. Then the percentage of stiffness allocation is varied between 0-100% and the results are studied. The optimal solution for stiffness is then selected and the shear force parameter is varied between 0-100%. This process gives a reasonable solution for the most advantageous distribution of stiffness and shear force and how they are allocated to different structural members. Though it is not a

comprehensive study and the stiffness parameter should be adjusted for every shear force value, this method shows several obvious trends that will aid in the design of hysteretic dampers for buildings.

The following examples illustrate the physical properties for the model building with 25% and 75% of building stiffness allocated to the secondary structure and primary structure, respectively, and 40% and 60% of shear force to secondary and primary, respectively. It will be shown momentarily why these values are chosen for this illustration.
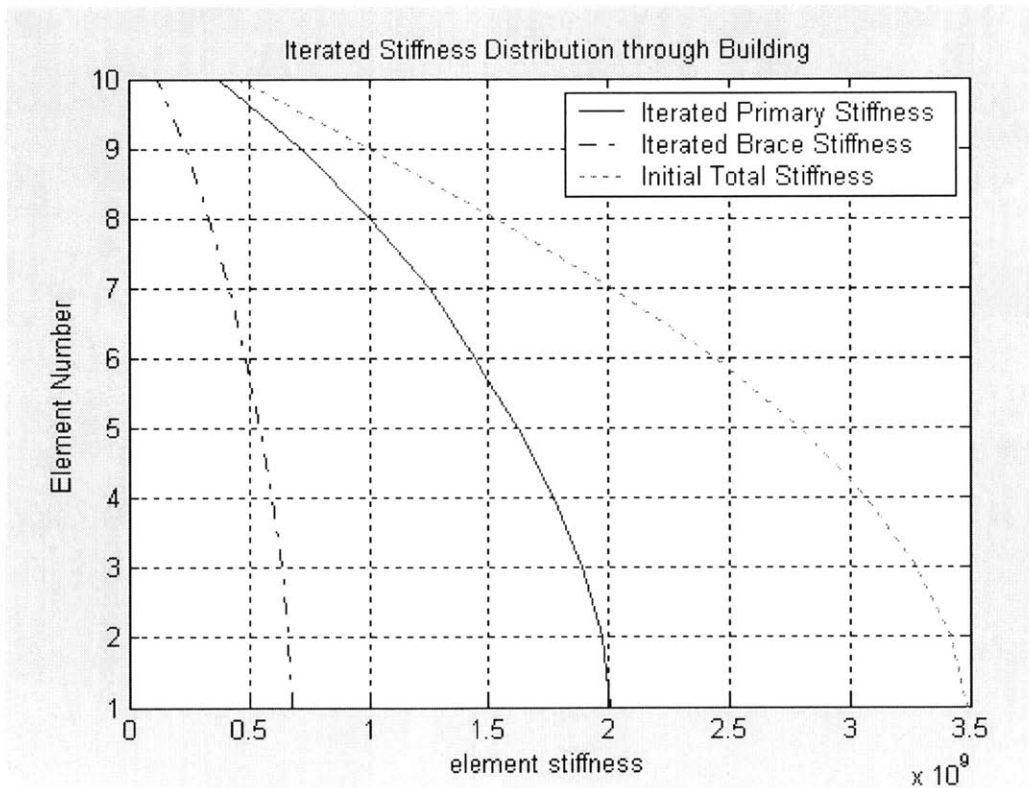
Figure 6-1: Stiffness Distribution of Building

Observe how the program takes the initial proposed stiffness distribution and converges on values for primary and brace stiffness. The final iterated total stiffness (secondary plus primary) is roughly 75% of the original guess. A second structural parameter the

program calculates is the yield force distribution in the braces and the shear force applied to the primary structural members, shown in Figure 6-2. Notice that the iterated yield shear force matches exactly the final shear force in the braces. This is physically realistic, since the hysteretic damper has no axial force capacity beyond yielding. Any force beyond this capacity must either go into the primary structure or be taken by the energy dissipation characteristics of the unbonded brace. This is shown by the overlapping of the 'iterated yield shear force' and 'maximum final shear force in braces' lines. Also notice that the ratio between Brace Shear Force and Primary Shear Force is not 40:60, as is specified. This is due to the fact that this allocation of shear force is specified and calibrated for the BSE-1, and the results shown are for maximum shear force experienced under BSE-2.
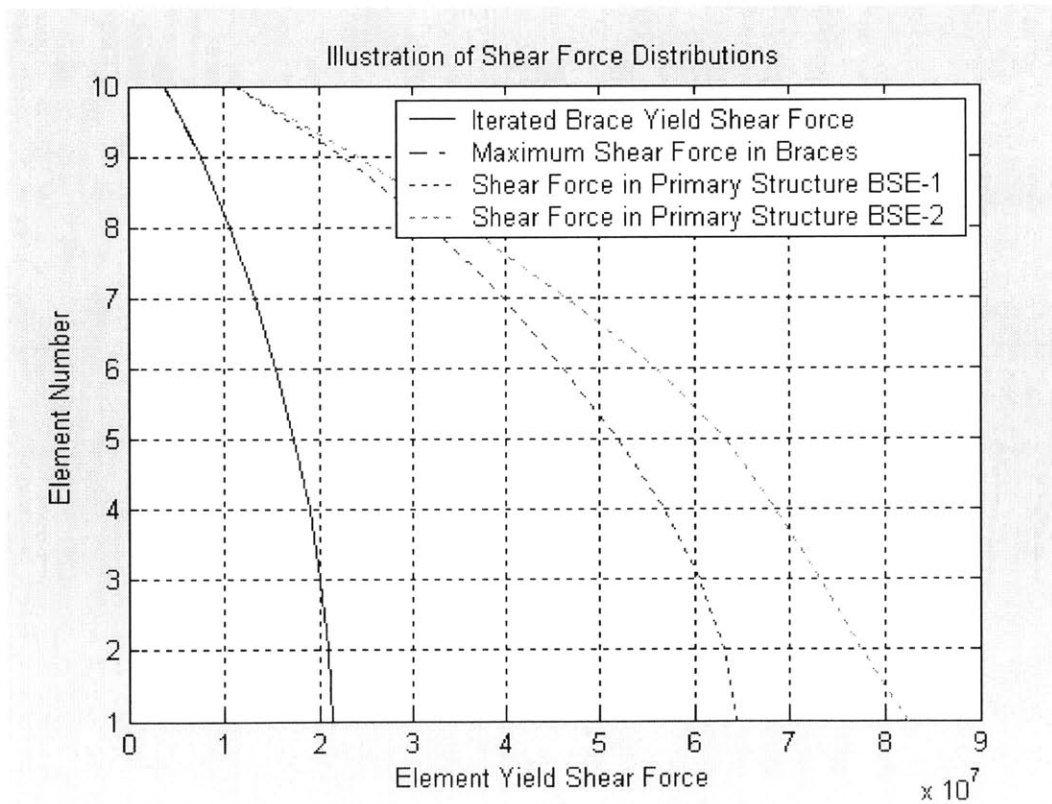

Figure 6-2: Shear Force Distribution of Building

Next is the calculated drift ratio throughout the building. The program outputs the drift associated with the original guess at stiffness, the drift associated with the iterated stiffness parameters, and finally the drift experienced under the extreme earthquake (BSE-2). Figure 6-3 illustrates the convergence on specified allowable drift, shown by the initial drift distribution and the 'drift-design earthquake' distribution. Observe that the allowable drift parameter, specified to be 0.02 meters (0.5% transient drift), is achieved with minor deviations. This occurs because only three iterations are performed for stiffness optimization. More iterations would result in complete convergence, however this requires significant computational power, which is still an obstacle even given current processing speeds. Three iterations are sufficient in this case because the achieved drift for BSE-1 is approximately 0.021 meters at the top story, which for the assumed 4-meter interstory height gives a drift percentage of 0.51 %, just slightly more than the desired 0.5%. The lower portion of the building, most important to the integrity of the building, is preserved. In addition, the structure remains elastic during the event, meaning the Immediate Occupancy Performance Level will be achieved.

Lastly, examine the drift associated with the BSE-2 earthquake, which is approximately 0.041 meters and relatively uniform throughout the building (slightly less at top and greater at bottom of structure). Such a magnitude is related to about 1.4% drift, slightly greater than the requirements proposed in this thesis to meet Life Safety Performance Level but still less than those proposed in *Guidelines*.
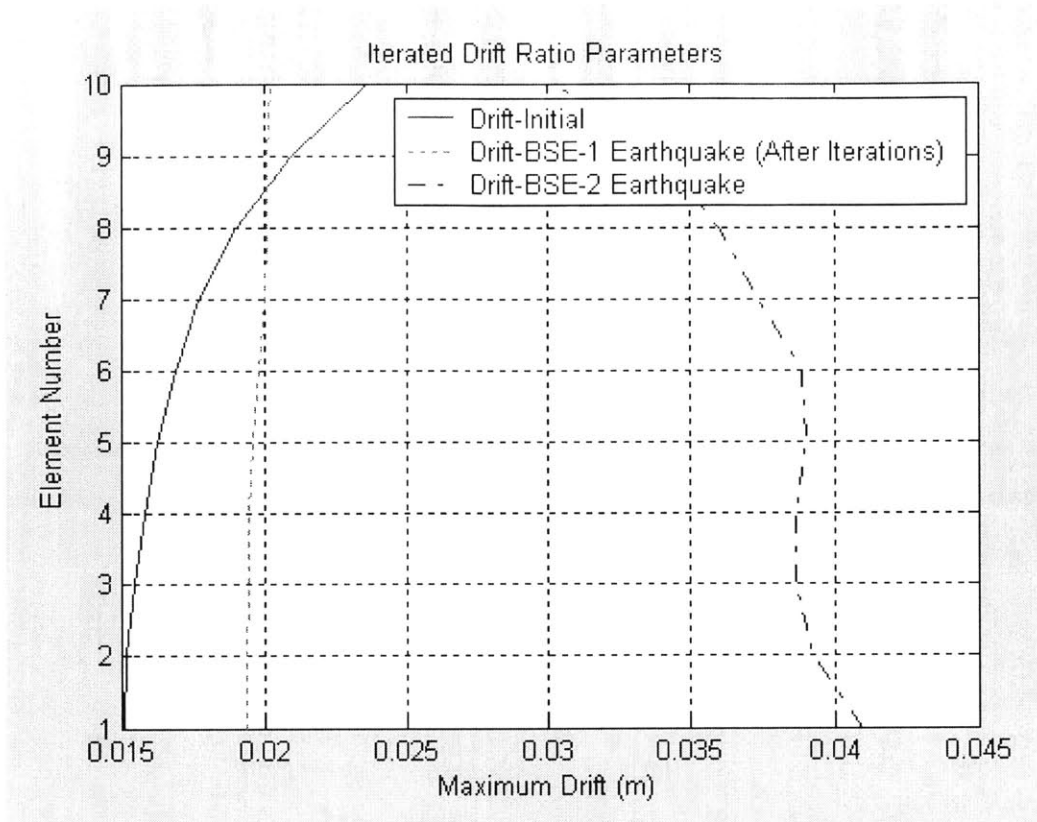
Figure 6-3: Drift of Building under BSE-1 & BSE-2 Earthquakes

The final parameter related to earthquake performance studied in this research is ductility demand. This parameter relates the deformation of a member to its inherent elastic limit, with a value greater than unity indicating the member is loaded beyond its elastic limit and anything less than one meaning total elastic response. Obviously ductility factors less than or equal to one are ideal, however values up to three are considered reasonable for earthquake response. Ductility demand greater than three is very high and the results could be catastrophic for a civil structure.

The ductility demand for this structure is extremely low for such an extreme seismic event. The structure is behaving elastically under the 75-year return earthquake and remains below the aforementioned ductility factor 3 for BSE-2. Note that the demand is much greater at or near the bottom of the structure, and this trend should be taken into

account when designing such a scheme. Furthermore, it is assumed that inelastic response occurs only for the braces. If the primary structure is designed to have a yield force greater than the primary shear force shown in Figure 6-2, than this assumption will indeed hold true.
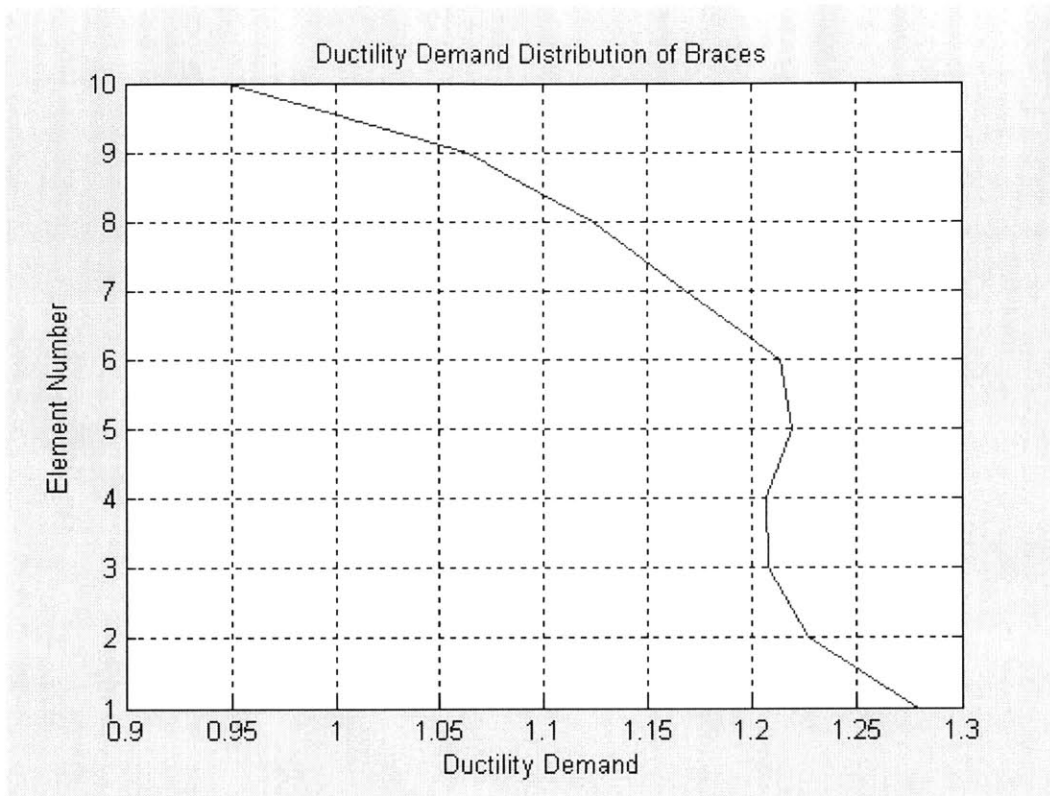
Figure 6-4: Ductility Demand of Braces under BSE-2 Earthquake

All this information on stiffness and yield force level versus response and demand is very informative, yet it still does not designate optimum design parameters. Though the drift distribution and ductility demand for this case (25% stiffness and shear force taken by the secondary structure) generally fall within design specifications, more questions need to be answered. Could the response be improved by tweaking the amount of required stiffness and shear force allocated to the primary and secondary structures? Is the structure too conservative and thus too expensive? The parametric study briefly

described at the beginning of this section seeks to answer these questions in a clear, organized manner.

6.1.2 Parametric Study

As a first conjecture, 25% brace stiffness and 25% brace shear is assumed in the structure. The percentage of brace shear is then held constant while percentage of brace stiffness is varied. Then an optimal stiffness allocation is selected and the shear force parameters are varied. "Optimal" is a fairly empirical term in most engineering problems, however it is defined as the most desirable or attractive solution in terms of performance and cost. Therefore, a performance/cost comparison must also be made. It is then up to the designer, owner, or developer to determine how to give weight to the various parameters and make a design selection. It is the goal of the author to objectively present the relationship between varying stiffness and shear force allocations to various structural performance parameters, namely drift and ductility demand. It is also important to consider how the performance relates to the relative cost of increasing or decreasing performance; therefore such a comparison is also made.

Refer to Figures 6-5a and 6-5b for results of varying the stiffness allocation parameter. Notice the obvious trend of the brace and primary stiffness being inversely related and equal at 50% (i.e. half of stiffness taken by secondary and half by primary structure). The structure always needs the same amount of total stiffness to resist seismic activity, regardless of where or how it is allocated. Perhaps the most important trend related to this aspect of the study is discrepancy in the maximum drift when stiffness allocation is varied. Initially increasing brace stiffness results in a decrease in drift until the structure responds within the allowable drift percentage (1%). However, too great an increase in allocated brace stiffness again increases the maximum drift above the desirable range. Thus, the amount of stiffness allotted to the secondary structure should be somewhere between 20%-60%.

Building Drift Trends for Varying Stiffness Allocations
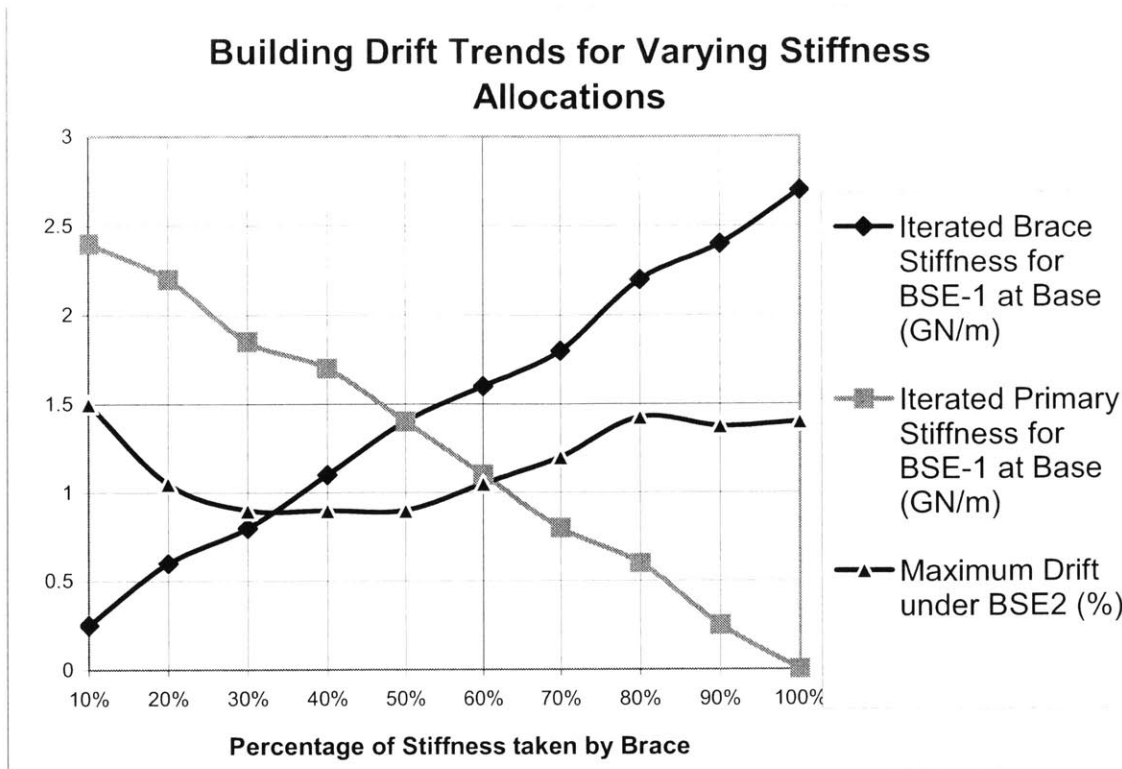
Figure 6-5a: Trends of Varying Brace/Primary Stiffness Ratio[7]

Before directly choosing 40% brace stiffness as a design value, which corresponds with minimum drift, one must also consider the ductility demand ratio associated with varying stiffness. Ductility demand increases in a quasi-parabolic fashion relative to increasing brace stiffness. Therefore it is justifiable to choose the lowest amount of brace stiffness that will meet the drift requirement. This is approximately 25%, equal to the original value used as a guess.

---

[7] Values for drift and ductility presented in Figures 6-5, 6-6 represent the absolute maximum throughout the height of the building and are not representative of any one particular element in the structure

Brace Ductility Demand Trends for Varying Stiffness Allocations
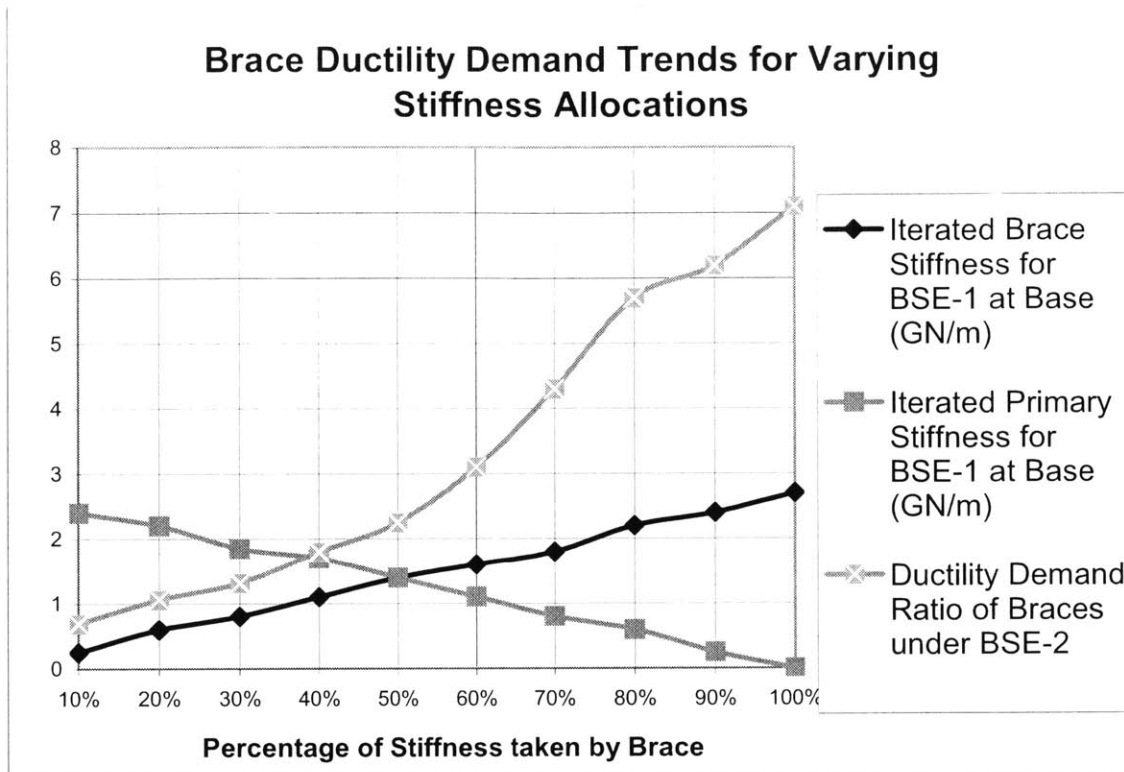
Figure 6-5b: Trends of Varying Brace/Primary Stiffness Ratio

With 25% brace stiffness allocation assumed for stiffness distribution, the shear force ratio is then varied. Stiffness is optimized to minimize both drift and ductility demand, and the allocation of shear force must be approached in a similar fashion. Figure 6-6a illustrates the maximum shear force the primary structure experiences and the yield shear force level in the unbonded braces during BSE-2. As the amount of brace shear force increases, the maximum ductility demand decreases. Observe the rapid decrease in ductility demand as bracing is initially added and then a gradual decrease as the percentage of brace shear force increases above 40%. In addition, these results indeed coincide with the basic physics of the problem: if the braces are designed to carry the majority of the shear force, the primary structure in turn has less demand. It appears that 40% brace shear force is optimal, as one can intuitively see a point of diminishing return with respect to ductility demand in this approximate region.

Shear Force Trends for 25% Brace Stiffness Allocation
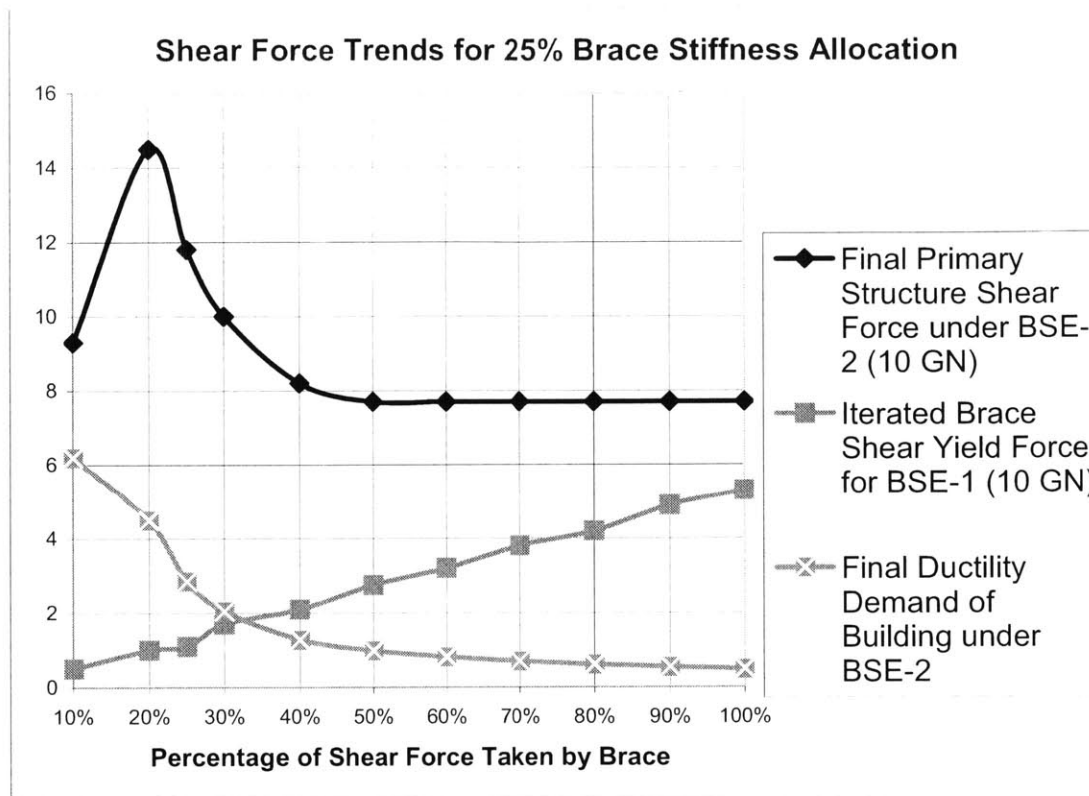
Figure 6-6a: Trends of Varying Brace Yield/Primary Shear Force Ratio[8]

To further illustrate the conjecture that anything beyond 40% brace stiffness is in fact too conservative, refer to Figure 6-6b. The brace shear yield force calculated by the program increases linearly, however at 40% brace shear force the magnitude of shear force levels off at 25 MN. This explains why, at 100% Brace Shear Yield Force, the primary shear force is not zero. Since the actually shear force in the braces is less than the calculated yield force, some shear force must be carried by the primary structure. Above this region the braces are over-designed, since the elements do not even begin to yield. Therefore the maximum shear yield force should be factored accordingly so as to ensure yielding and integrate the energy dissipation characteristics of the dampers. Given the results presented in Figures 6-6a and 6-6b, it is thus wise to choose 40% brace shear force ratio.

---

[8] Trends based on a slightly tighter drift tolerance of 0.3%

Shear Force Trends for 25% Brace Stiffness Allocation
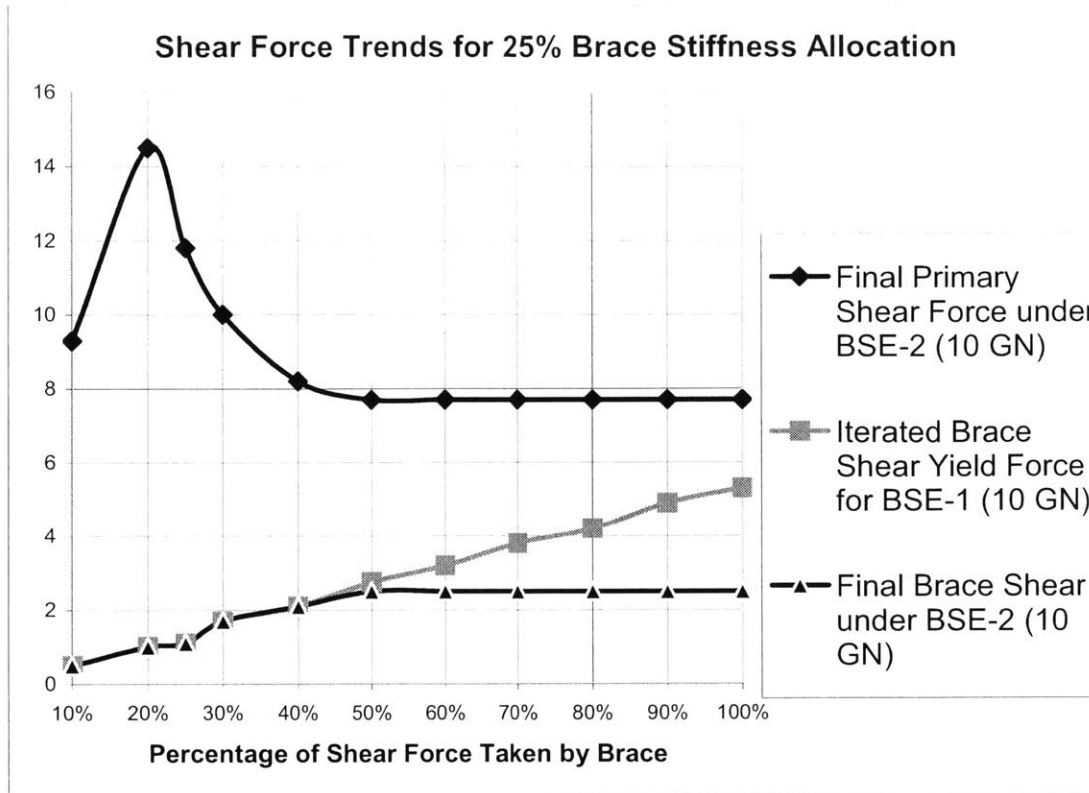
Figure 6-6b: Trends of Varying Brace Yield/Primary Shear Force Ratio

All of the above results lead to a general conclusion that a 10-story building designed for Life Safety Performance Level under BSE-2 should have a brace stiffness to primary stiffness ratio of 0.25 and a brace shear yield force to primary shear force of 0.40. The complete results for this scenario (the optimal design solution) are shown in Figures 6-1 through 6-4. Next is a feasibility study to explore whether these design values are even reasonable or achievable with existing or potential technologies.

6.2 Feasibility Study

Given the necessary stiffness, yield force level, and drift in the structure, it is vital to study the potential of realizing this design methodology in a physical structure. With the

25/40 distribution (25% stiffness and 40% shear force to braces), the maximum stiffness is 7×10^5 kN/m. The following figure illustrates a typical bracing scheme used in civil structures, and since the braces provide stiffness only in the axial direction, the total necessary stiffness must be divided by the cosine of the angle of the brace. Therefore the total necessary brace stiffness at the bottom floor is approximately 1×10^6 kN/m, which translates to 5710kip/in [14]. This necessitates the use of approximately 10 of the prototype KCI braces (stiffness equal to 335 kip/in) that are currently being tested. The use of stiffer Nippon Steel braces would require fewer braces.

(b)
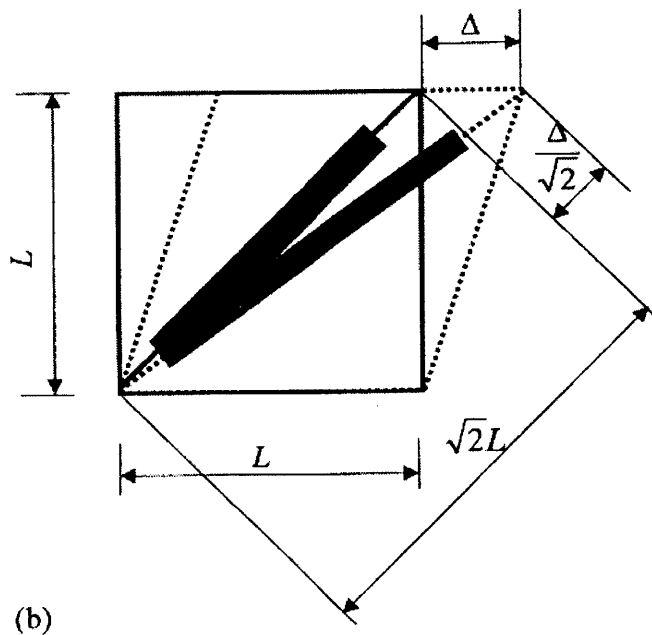
Figure 6-7: Typical Brace Configuration and Geometry [6]

Perhaps a more important parameter to consider is the yield force level. At the base of the structure, the calibrated yield force level is 2×10^7 N, or 4500 kip. Again, since the braces will be attached at a 45-degree angle, the yield force requirement is approximately 6400 kip. Using the 500 kip yield force Nippon Steel braces the number of required braces is 12, and specifying KCI braces would require slightly more. Thus, yield force level is indeed the controlling design parameter when actually implementing this methodology. Please see Appendix B for calculations used in this brief analysis. It

should be noted that 8-12 braces is not unreasonable for a large structure, and given the relatively small nature of the braces this may not be too great an impedance on architectural features. Figure 6-8 shows the response of a brace equivalent to summing all of the requisite 12 braces. The necessary displacement is roughly three times the elastic limit of the member, which is extreme but conceivable. Examine Figure 4-1, the hysteresis loop of the KCI prototype. In this case the specimen yields nearly 4.7 times its elastic limit, approximately 30% more than is required in this design scheme.
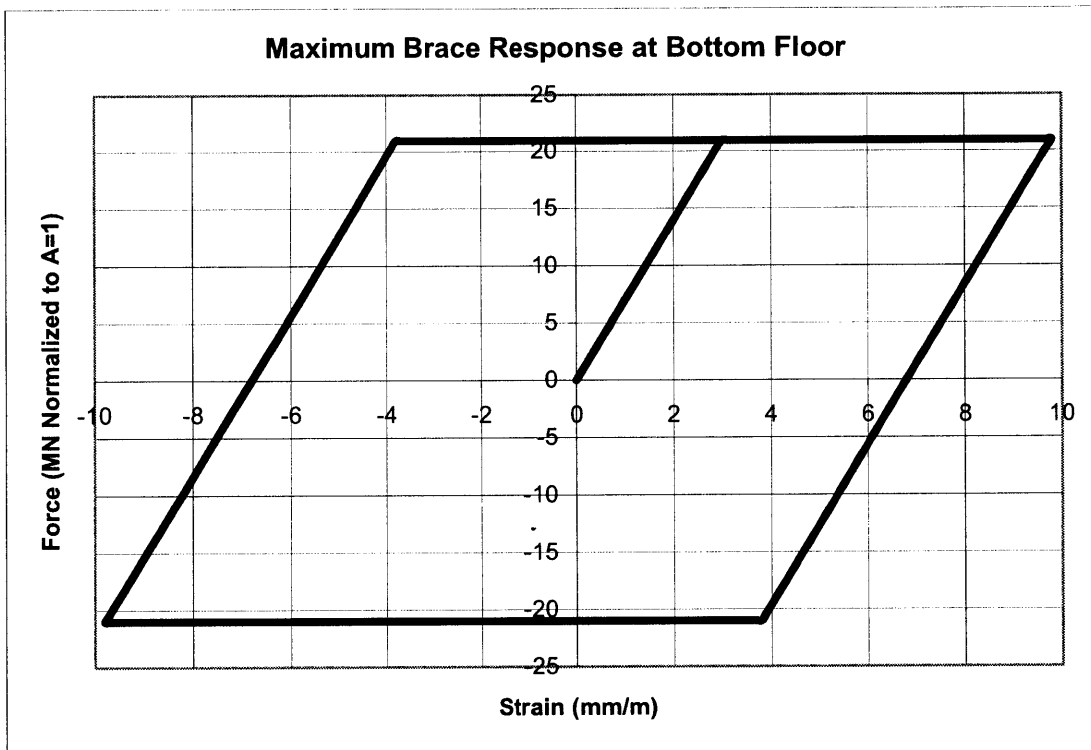
Figure 6-8: Brace Response at Bottom Floor

In addition, this analysis is for the bottom story of the structure, where stiffness and strength are the greatest, whereas the top story (6×10^6 N) requires only 4 typical Nippon Steel braces. In this case, where the structure is relatively tall, the earthquake is large, and the performance design constraints are extremely stringent, the stiffer, high yield force brace schemes seem most applicable. This is a highly qualitative approach to studying the

feasibility of the results of this research, however it demonstrates the potential that this approach has for real-world application.

Chapter 7

Cost

Finally, and perhaps most importantly, is a relative cost analysis for allocation of stiffness throughout the building. While it is important to allocate and calibrate the optimal stiffness both in the bracing and primary structures, it is equally important to assess the cost of doing so. Since the stiffness of the brace depends on its axial capacity, stiffness and thus cost vary linearly with increasing stiffness. However, it has been shown that the cost of lateral stiffness for a frame system varies with the square of the cross-sectional area, or in a quasi-parabolic fashion [13]. The following figure shows the total cost of stiffness in terms of the amount of material required (normalized) for variable brace/primary stiffness ratios. Since brace stiffness varies linearly with amount of material, it should follow that allocating 100% stiffness to braces would be the least expensive, while the opposite would be true for 100% primary stiffness. This intuition coincides with the results of the simulation.
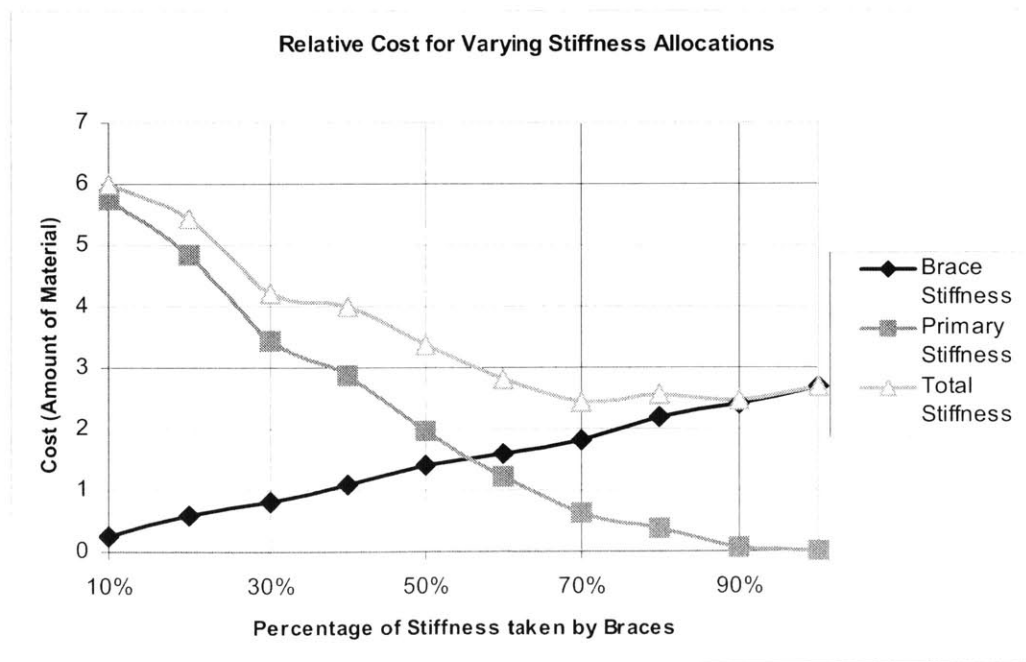

Figure 7-1: Relative Cost of Stiffness

With this study it is then possible to investigate the optimal stiffness distribution in a different way, in terms of cost and drift experienced under BSE-2. Figure 6-10 shows the drift-cost parameter for various stiffness allocations. To calculate the drift-cost parameter, total relative cost is multiplied by the maximum drift experienced under an extreme seismic event, and the results are normalized to one.

Cost-Performance for Varying Stiffness Allocations
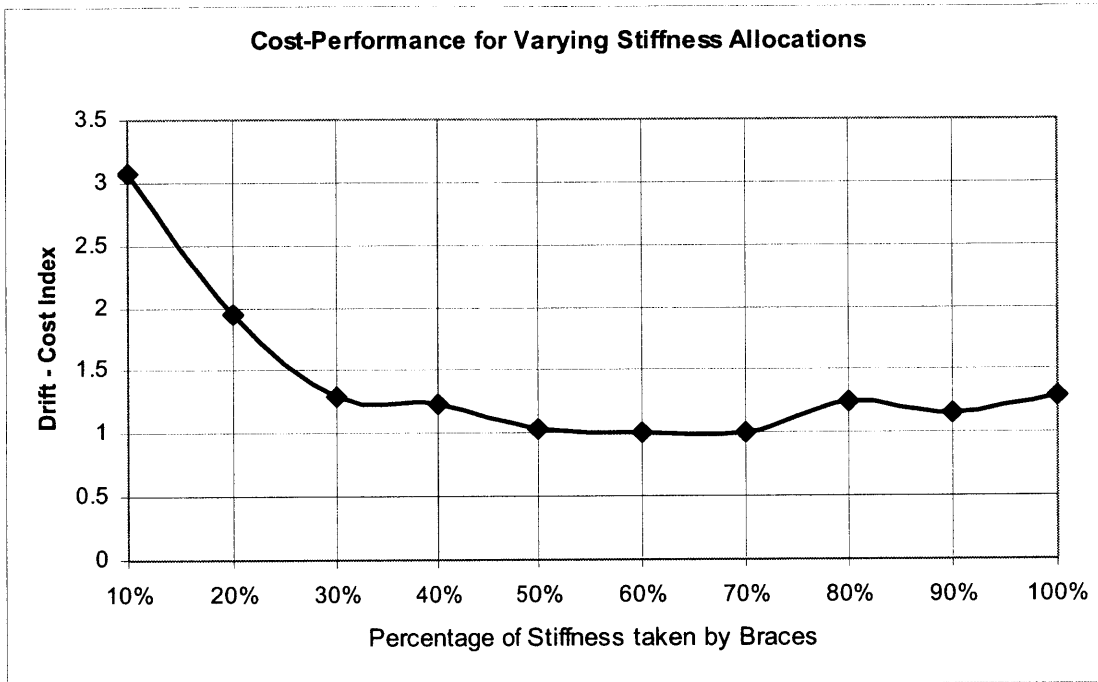
Figure 7-2: Drift-Cost Parameter

With this data it is apparent that in terms of cost and maximum drift the most efficient distribution occurs between 60%-70% relative brace damping. However, Figure 6-5b shows that at 70% the ductility demand of the structure exceeds 4, which is generally unacceptable. Refer to the discussion in Section 6.1.2. Notice that 25% brace stiffness results in approximately 50% increase in cost in terms of this index. The designer must prioritize the design parameters to optimize the structure of the building in terms of response and cost, and in the case presented in 6.1.2 priority is given purely to structural response. However, if one considers cost as well it is certainly viable to increase the brace stiffness allocation in order to minimize cost. This jeopardizes the performance criteria described in this thesis, and the conservative design approach proposed in

Chapter 6 would be abandoned. In this case it would also be wise to increase the allowable drift, a parametric study in its own right, to be less conservative. This allows for an overall decrease in stiffness and thus a decrease in structural cost.

Chapter 8

Conclusions

Performance of buildings during past earthquakes and developing technologies in the construction industry are rendering the current strength-based seismic design codes insufficient. It has been shown in several publications and argued strongly here that the motion-based design approach is the wave of the future in structural design. By constraining the motion of a building to a certain specification, the engineer can design a structure that meets or exceeds the Performance Levels proposed as mandatory by the Federal Emergency Management Agency. Where valid earthquake data is present, as is the case on the West Coast, in Japan, and in other highly seismic areas, the use of time-history analysis is not simply an important supplement to equivalent static analysis procedures but necessary to obtain satisfactory design.

With the growing trend towards motion-based design and performance-based assessment of structural efficiency, there now exists huge potential for the use of hysteretic dampers in buildings. With increasing research and development both into material behavior and more global system behavior, the market would only seem to get larger. The use of hysteretic dampers for damage-controlled structures is already well under way in Japan and is growing in the United States. Without a consistent, robust design methodology however, the growth of using hysteretic dampers domestically could be stifled. This thesis has presented a thorough design methodology that is easily repeatable and could be introduced to more conventional seismic design.

Presented in Chapters 5, 6 and 7 is the basic theory, performance constraints, and iterative algorithm used to converge on the "optimal" design. Under the Northridge 1994 earthquake, a 500 year return event, the allocation of 25% of stiffness to the hysteretic dampers and 75% to the primary structure achieves the Performance Level goals described in Section 5.2. Additionally, 40% and 60% of horizontal shear force is

allocated to the braces and primary structure, respectively. By setting the shear yield force in the braces equal to the brace shear force experienced under BSE-1, the braces yield under BSE-2 and the overall structure reaps the benefits of the damping properties of hysteresis. Further research into response under different earthquakes, comparison studies relative to undamped structures, and cost studies with respect to varying allowable drift and ductility demand constraints would nicely supplement this work.

References

[1]   ASCE: <u>Minimum Design Loads for Buildings and Other Structures</u>. Reston, VA: American Society of Civil Engineers, 2000.

[2]   Connor, Jerome J. <u>Introduction to Structural Motion Control</u>, Prentice Hall, 2003

[3]   Connor, J.J.; Wada, A.; Iwata, M.; Huang, Y.H. "Damage-Controlled Structures. I: Preliminary Design Methodology for Seismically Active Regions", <u>Journal of Structural Engineering</u>, April 1997.

[4]   Tokyay, Borah. <u>A Design Methodology for Hysteretic Dampers</u>, Massachusetts Institute of Technology, June 2002.

[5]   FEMA-273: <u>NEHRP Guidelines for the Seismic Rehabilitation of Buildings</u>. Technical Report, Federal Emergency Management Agency, 1997.

[6]   Wada, Akira; Huang, Yi-Hua; Iwata, Mamoru. "Passive Damping Technology for Buildings in Japan", <u>Prog. Struct. Engng Mater</u>. 2000; 335-350.

[7]   United States Geological Survey Earthquake Records.

[8]   Automated Production of Low Cost Pultruded Composite Bracing for Seismic Energy Dissipation Structures Phase II SBIR Mid-Term Review, March 19, 2003.

[9]   Clark, Peter; Aiken, Ian; Ko, Eric; Kasai, Kazuhiko; Kimura, Isao. "Design Procedures for Buildings Incorporating Hysteretic Damping Devices".

[10]   Clark, Peter W.; Aiken, Ian D.; Nakashima, Masayoshi; Miyazaki, Mitsuo; Midorikawa, Mitsumasa. "New Design Technologies", <u>Lessons Learned Over Time, Learning From Earthquakes, Volume III</u>, 1999.

[11]   Yamaguchi, Hiroki and El-Adb, Ashraf. "Effect of earthquake energy input characteristics on hysteretic damping efficiency", Earthquake Engng Struct. Dyn. 2003; 827-843.

[12]   FEMA-355C: Systems Performance of Steel Moment Frames Subject to Earthquake Ground Shaking. Technical report, Federal Emergency Management Agency, 2001.

[13]   Schueller, Wolfgang. The Vertical Building Structure, Van Nostrand Reinhold, New York, 1990.

[14]   http://www.megaconverter.com/

Appendix A Ground Motion Records [12]

Table A-2 Basic Characteristics of Los Angeles Ground Motion Records

50/50 Set of Records (72 years Return Period)						
Designation	Record Information	Duration (sec)	Magnitude Mw	R (km)	Scale	PGA (in/sec^2)
LA41	Coyote Lake, 1979	39.38	5.7	8.3	2.28	227.7
LA42	Coyote Lake, 1979	39.38	5.7	8.3	2.28	128.7
LA43	Imperial Valley, 1979	39.08	6.5	1.2	0.40	55.4
LA44	Imperial Valley, 1979	39.08	6.5	1.2	0.40	43.1
LA45	Kern, 1952	78.60	7.7	107.0	2.92	55.7
LA46	Kern, 1952	78.60	7.7	107.0	2.92	61.4
LA47	Landers, 1992	79.98	7.3	64.0	2.63	130.4
LA48	Landers, 1992	79.98	7.3	64.0	2.63	118.8
LA49	Morgan Hill, 1984	59.98	6.2	15.0	2.35	123.0
LA50	Morgan Hill, 1984	59.98	6.2	15.0	2.35	211.0
LA51	Parkfield, 1966, Cholame 5W	43.92	6.1	3.7	1.81	301.4
LA52	Parkfield, 1966, Cholame 5W	43.92	6.1	3.7	1.81	243.8
LA53	Parkfield, 1966, Cholame 8W	26.14	6.1	8.0	2.92	267.7
LA54	Parkfield, 1966, Cholame 8W	26.14	6.1	8.0	2.92	305.1
LA55	North Palm Springs, 1986	59.98	6.0	9.8	2.75	199.8
LA56	North Palm Springs, 1986	59.98	6.0	9.8	2.75	146.3
LA57	San Fernando, 1971	79.46	6.5	1.0	1.30	97.7
LA58	San Fernando, 1971	79.46	6.5	1.0	1.30	89.2
LA59	Whittier, 1987	39.98	6.0	17.0	3.62	296.7
LA60	Whittier, 1987	39.98	6.0	17.0	3.62	184.7

10/50 Set of Records (475 years Return Period)						
Designation	Record Information	Duration (sec)	Magnitude Mw	R (km)	Scale	PGA (in/sec^2)
LA01	Imperial Valley, 1940	39.38	6.9	10.0	2.01	178.0
LA02	Imperial Valley, 1940	39.38	6.9	10.0	2.01	261.0
LA03	Imperial Valley, 1979	39.38	6.5	4.1	1.01	152.0
LA04	Imperial Valley, 1979	39.38	6.5	4.1	1.01	188.4
LA05	Imperial Valley, 1979	39.08	6.5	1.2	0.84	116.4
LA06	Imperial Valley, 1979	39.08	6.5	1.2	0.84	90.6
LA07	Landers, 1992	79.98	7.3	36.0	3.20	162.6
LA08	Landers, 1992	79.98	7.3	36.0	3.20	164.4
LA09	Landers, 1992	79.98	7.3	25.0	2.17	200.7
LA10	Landers, 1992	79.98	7.3	25.0	2.17	139.1
LA11	Loma Prieta, 1989	39.98	7.0	12.4	1.79	236.9
LA12	Loma Prieta, 1989	39.98	7.0	12.4	1.79	114.4
LA13	Northridge, 1994, Newhall	59.98	6.7	6.7	1.03	261.8
LA14	Northridge, 1994, Newhall	59.98	6.7	6.7	1.03	253.7
LA15	Northridge, 1994, Rinaldi	14.95	6.7	7.5	0.79	206.0
LA16	Northridge, 1994, Rinaldi	14.95	6.7	7.5	0.79	223.9
LA17	Northridge, 1994, Sylmar	59.98	6.7	6.4	0.99	219.9
LA18	Northridge, 1994, Sylmar	59.98	6.7	6.4	0.99	113.3
LA19	North Palm Springs, 1986	59.98	6.0	6.7	2.97	193.3
LA20	North Palm Springs, 1986	59.98	6.0	6.7	2.97	180.9

2/50 Set of Records (2475 years Return Period)						
Designation	Record Information	Duration (sec)	Magnitude Mw	R (km)	Scale	PGA (in/sec^2)
LA21	1995 Kobe	59.98	6.9	3.4	1.15	495.3
LA22	1995 Kobe	59.98	6.9	3.4	1.15	353.4
LA23	1989 Loma Prieta	24.99	7.0	3.5	0.82	361.4
LA24	1989 Loma Prieta	24.99	7.0	3.5	0.82	362.6
LA25	1994 Northridge	14.95	6.7	7.5	1.29	335.3
LA26	1994 Northridge	14.95	6.7	7.5	1.29	364.3
LA27	1994 Northridge	59.98	6.7	6.4	1.61	357.8
LA28	1994 Northridge	59.98	6.7	6.4	1.61	513.4
LA29	1974 Tabas	49.98	7.4	1.2	1.08	312.4
LA30	1974 Tabas	49.98	7.4	1.2	1.08	382.9
LA31	Elysian Park (simulated)	29.99	7.1	17.5	1.43	500.5
LA32	Elysian Park (simulated)	29.99	7.1	17.5	1.43	458.1
LA33	Elysian Park (simulated)	29.99	7.1	10.7	0.97	302.1
LA34	Elysian Park (simulated)	29.99	7.1	10.7	0.97	262.8
LA35	Elysian Park (simulated)	29.99	7.1	11.2	1.10	383.1
LA36	Elysian Park (simulated)	29.99	7.1	11.2	1.10	424.9
LA37	Palos Verdes (simulated)	59.98	7.1	1.5	0.90	274.7
LA38	Palos Verdes (simulated)	59.98	7.1	1.5	0.90	299.7
LA39	Palos Verdes (simulated)	59.98	7.1	1.5	0.88	193.1
LA40	Palos Verdes (simulated)	59.98	7.1	1.5	0.88	241.4

Appendix B: Feasibility Calculations
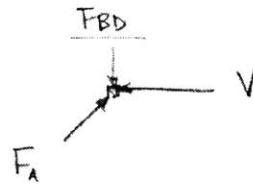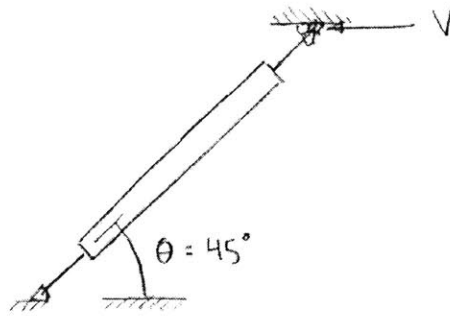
$F_A \cos\theta = V$

$F_A = \dfrac{V}{\cos\theta}$

$V = \dfrac{V_T}{\alpha}$

$V_{T,BASE} = 2 \times 10^7 N = 4500 \, kip$

$V_{T,TOP} = 0.6 \times 10^7 N = 1350 \, kip$

$\longrightarrow F_{A,BASE} = \dfrac{4500 \, kip}{\alpha \cos 45} \cong \dfrac{6400 \, kip}{\alpha}$

$\longrightarrow F_{A,TOP} = \dfrac{1350 \, kip}{\alpha \cos 45} \cong \dfrac{1900}{\alpha} \, kip$

USING $F_Y = 500 \, kip$ BRACES

$\alpha = \dfrac{F_A}{F_Y}$

$\alpha_{BOTTOM} = 12.8 \longrightarrow 13$ BRACES

$\alpha_{TOP} = 8 \longrightarrow 4$ BRACES